HHS Public Access

Author manuscript

Anal Chem. Author manuscript; available in PMC 2019 January 02.

Published in final edited form as:

Anal Chem. 2018 January 02; 90(1): 19–39. doi:10.1021/acs.analchem.7b04251.

Surface Plasmon Resonance: Material and Interface Design for Universal Accessibility

Samuel S. Hinman[†], **Kristy S. McKeating**[‡], and **Quan Cheng**[*,†,‡]

[†]Environmental Toxicology, University of California–Riverside, Riverside, California 92521, United States

[‡]Department of Chemistry, University of California–Riverside, Riverside, California 92521, United States

The ability to monitor biomolecular reactions in a real-time and label free manner is nearly synonymous with the surface plasmon resonance (SPR) technique. At its basis, SPR relies on the interaction of an incoming light source with a thin metallic film in close contact with a prism or grating, which under the correct experimental conditions, allows for the propagative oscillation of the conduction electrons at the surface of the metallic material. Termed surface plasmon polaritons (SPPs), these oscillating, electromagnetic fields are extremely sensitive to small changes in the refractive index within the dielectric near the sensing interface, where various binding events and interactions can be detected. It is essential to note that the term, surface plasmon resonance, can refer to two distinct forms of the phenomenon, in which the electromagnetic fields propagate along a planar surface (i.e., SPPs) or in which they are localized to a nanostructure smaller than the incident wavelength (i.e., localized surface plasmons). The topic of localized surface plasmon resonance (LSPR) has drawn great attention, meriting its own discussions, and has been extensively reviewed elsewhere.[1–6] The discussion herein will focus solely on the utilization of the propagating form (i.e., SPPs) and in a modern context.

Historically, SPR has seen its predominant use within pharmaceutical research, where commercial instrumentation has been employed for drug discovery, antibody characterization, and studies of protein/enzyme inhibition. Recent advances in instrumentation and plasmonic materials, however, are rapidly expanding the environments in which SPR can be employed. The options for designing an appropriate instrument and sensing interface are vast, such that SPR can now be tailored to an extraordinary variety of applications, whether they be in a research laboratory, the local hospital, or the field for environmental research. As such, the number of publications in the field has undergone substantial growth, with those on topics that include the keywords “surface plasmon resonance” exceeding 3000 per year since 2014 (Figure 1). There have recently been a

[*]**Corresponding Author** Tel: (951) 827-2702. Fax: (951) 827-4713. quan.cheng@ucr.edu.

Special Issue: Fundamental and Applied Reviews in Analytical Chemistry 2018

ORCID Samuel S. Hinman: 0000-0002-7727-0450
Quan Cheng: 0000-0003-0934-358X

Notes

The authors declare no competing financial interest.

number of excellent reviews focused on the various applications in which SPR spectroscopy and its derivatives can be employed,[7–11] and therefore, within this Review, we discuss SPR from a design perspective, covering the various instrumental and interfacial aspects that have been created and optimized only within the past couple of years in order to highlight the increased accessibility of this platform to a wider range of scientific researchers and disciplines.

PLATFORMS AND INSTRUMENTATION

The introduction of the BIAcore instrument to the mass market in 1990 marked a significant milestone for scientists interested in label-free optical sensing, as surface plasmon resonance (SPR) was made available to a wide audience of researchers with varying technical backgrounds for the first time.[12] This product line currently represents one of the largest shares of commercial SPR instrumentation, and many aspects of the technology remain the same: a gold coated sensor chip is inserted over an optical coupler within a housing unit that also contains a light source, polarizer, detector, and integrated sample handling fluidics. The measurements taken under these setups are heterogeneous, with recognition elements immobilized to the gold film and respective binding partners flowed over to monitor concentrations and binding kinetics in real time. While these basic instrumental design motifs are all present in modern SPR instrumentation, variations in optical geometries and components have grown massively, expanding the versatility of this technique within the areas of high-throughput screening, nanoscale visualization, and clinical/field diagnostics.

From a physical perspective, SPR is the result of a momentum transfer from an electromagnetic source (e.g., light) to the delocalized electrons of a bulk metal, thereby causing those electrons to oscillate in resonance with the incident light at the metal/dielectric interface. The coupling of incident light to a metal's conduction electrons is only possible when the wavevector of incident light (k_0) is equal to the wavevector of the surface plasmon polaritons (SPPs) generated (k_{sp}), as defined below:

$$k_{sp} = K_0 \sqrt{\frac{\varepsilon_m(\lambda)\varepsilon_s(\lambda)}{\varepsilon_m(\lambda) + \varepsilon_s(\lambda)}}$$

where λ is the wavelength of light, ε_m is the complex dielectric constant of the metal, and ε_s is the complex dielectric constant of the surrounding medium. Due to the dependency of k_{sp} on the dielectric constants, ε_m and ε_s, $k_{sp} \neq k_0$ when light is freely propagating through a vacuum, and the resonant conditions will not be satisfied. The instruments outlined in this section, including Kretschmann configuration setups, SPR microscopes, fiber optic platforms, and portable instruments, each provide a means to make up for this mismatch in momentum, with respective advantages that have been leveraged in powerful ways over the past several years (Figure 2).

Kretschmann Configuration

Kretschmann and Raether were successful in exciting surface plasmon waves at a silver/air interface under attenuated total reflection (ATR) geometry, which today is referred to as the

Kretschmann configuration for SPR (Figure 2A).[13] Under this experimental setup, the light source, coupling prism, metal film (e.g., gold or silver), and detector are arranged in reflectance geometry, with spectra of reflected light monitored in real-time. By coupling light through a high refractive index prism in this configuration, the effective wavevector of incident light (k_{eff}) is increased according to the equation below:

$$k_{\mathrm{eff}} = k_0 n_{\mathrm{D}} \sin(\theta) = \frac{2\pi}{\lambda} n_{\mathrm{D}} \sin(\theta)$$

where n_{D} is the refractive index of the prism and θ is the angle of incidence. Under this setup, not only may k_{sp} equal k_{eff}, allowing for surface plasmon polariton (SPP) generation, but also coupling conditions may be tuned through variations in the wavelength (λ) or incident angle (θ) of the light source.

The optimal condition under which SPR occurs manifests as a dip in the reflectance spectrum of the material, which will shift in accordance with changes in n or ε_{s}. Changes in the reflectance spectrum of an SPR sensor in the Kretshmann configuration can be monitored through shifts in the minimum angle, wavelength, intensity, or phase of outgoing light while the system is under angular or wavelength interrogation. For example, a commercial white light source, birefringent quartz crystal, sheet polarizer, and fiber optic spectrometer can be arranged in conjunction with an equilateral prism and gold film to monitor phase shifts in outgoing light during sensor calibration, which results in lower detection limits, but also lower dynamic ranges, compared to the other interrogation and detection methods.[14,15] Alternatively, the white light source, sheet polarizer, and spectrometer can be used in conjunction with a gold-coated dove prism for a more accessible optical setup and maximum portability.[16–20] These instrumental parameters can have major impacts on the physical footprint of the instrument and sensor performance, and therefore, the choice of interrogation and detection methods should be taken into account during assay design according to the intended usage of the setup.

Multimodal Spectroscopy—With instrumental designs becoming more diverse and sophisticated, the ability to simultaneously interrogate multiple parameters has grown, thus allowing for greater understandings of complex systems. It is well established that SPR signals can be affected by environmental factors beyond the refractive index, including temperature[21,22] and charge,[23,24] which can render discrimination of true analyte signal difficult. The utilization of a dual-angle measurement technique has been proposed to simultaneously discriminate changes in refractive index and temperature on an SPR device in the Kretschmann configuration.[25] Under this method, the intensity of reflected light is measured at two different angles, one below the SPR angle and one above, which respond variably to refractive index and temperature. An inverse sensitivity matrix, which defines the refractive index and temperature sensitivities at each angle, may then be applied to both angular measurements for discriminatory extrapolation of refractive index and temperature changes. This technique could conceivably be applied toward other sources of signal drift, provided that the reflected light intensities respond variably at different measurement angles or wavelengths, thereby diminishing signal drift arising from ambient interferences at the instrumental design level.

Similar approaches may be applied for accurate determination of particle size, concentration, and deformation at an SPR sensor interface. While dual-wavelength interrogation techniques have existed for many years,[26–29] Rupert et al. were the first to provide a thorough treatment of experimental data toward highly accurate shape characterizations for adsorbed nanoparticles.[30] The utilization of multiple interrogation wavelengths allowed for SPPs exhibiting different bulk solution penetration depths, for which the respective sensor responses could be treated in a ratiometric manner to extract adsorbed particle size. These methods were applied toward characterization of polystyrene beads, synthetic lipid vesicles, and extracellular vesicles with a size accuracy of ±5%. Combined with nanoparticle tracking analysis (NTA) and with adsorbed vesicle deformation taken into account, subpopulations of CD63-positive extracellular vesicles could be isolated on the sensor surface, and their respective concentrations within complex media were established within <10% error. Such methods not only allow for affinity-based analysis with SPR sensors but also make the technique size and shape selective.

Imaging—Surface plasmon resonance imaging (SPRi) is a high-throughput and label-free characterization technique based on the Kretschmann configuration for SPR, in which a laterally expanded light source, either a laser or LED,[31] is used for SPP excitation across an array, and a CCD camera is used for digital image acquisition to monitor the intensity of reflected light from each array element (Figure 2B). Like spectroscopic SPR sensors, SPRi measurements are also sensitive to both refractive index and temperature and thus inherit many of the advantages and disadvantages from the aforementioned technique.[32] Numerous reviews have been published on SPRi alone, with Spoto and Minunni highlighting technological developments since the early 2000s, including nanomaterial integrations and requirements for widespread adaptation.[33] Advances in surface chemistries for ultrasensitive detection of nucleic acids and proteins were reviewed by Fasoli and Corn, with emphases placed on nucleic acid enzymes and nanoparticles for effective signal amplication.[34] Since these reviews were published, SPRi has been further applied toward the detection of ABH antigen,[35] matrix metalloproteinase-1,[36] and EGFR expression,[37] in addition to various cancer protein,[38] saccharide,[39] virus,[40] RNA,[41] and mRNA[42] targets. Newly developed printing protocols, including microwell[43] and trehalose-assisted[44] methods, have also been demonstrated for SPRi, which are certain to enhance both sample handling and characterization of target molecules that require stringent hosting environments. Beyond multiplexed array detection, SPRi has been applied toward the study of bacterial films, adhesion, and mobility using the visualization capabilities offered by the technique.[45–47]

Advances in SPRi instrumentation have ranged from the conservative, yet undoubtedly important end, with integrated temperature control and monitoring demonstrated,[48,49] to the more radical, including variations on traditionally used monochromatic light sources and CCD cameras. Researchers desiring both the high dynamic ranges of spectroscopic SPR and the throughput capabilities of SPRi have sought after technical solutions that allow for both, with their studies converging on wavelength interrogation for collected array images. Sereda et al. propose a multispectral setup that utilizes 5 LEDs of various color for excitation.[50] As these light sources are sequentially lit, images for each are generated which can be analyzed for the construction of location-specific wavelength reflectivity curves, with the

measurement time of each being ca. 10 s. Shao and co-workers were able to streamline this setup through the use of a white light source and a liquid crystal tunable filter (LCTF), which is capable of selectively allowing specific wavelengths of light to pass through and is electronically controlled.[51,52] Acquisition of wavelength reflectivity curves were minimized to 700 ms and later to 350 ms through use of an acousto-optic tunable filter (AOTF).[53] While these spectral imaging approaches have significantly advanced the versatility of SPRi, their integration into conventional SPRi instrumentation is limited by the high price of LCTFs and AOTFs, for which any increase in SPRi performance has yet to be established empirically. However, the concern about cost will likely be assuaged in the near future provided that the manufacturing and demand for these components increase.

SPR Microscopy

While SPR has not traditionally been considered as a nanoscale visualization technique, developments in SPR microscopy (SPRM) are rendering it a powerful tool for location-specific characterizations down to the single particle and single molecule level. Numerous SPRM setup designs exist, including utilization of an objective lens with a prism coupler[54] and local excitation of SPPs through a high numerical aperture (NA) objective.[55] The current platform of choice, however, utilizes a high NA objective to guide collimated light from a laser source, reflecting it off the back focal plane of the objective and exciting SPPs at a high incident angle with respect to a gold film just beyond the objective lens, before finally collecting the reflected SPR image (Figure 2C).[56] Binding events appear as bright points in the image, connected to significantly larger parabolic tails resulting from scattering of SPPs in the direction of their propagation. These tails allow for indirect visualization of objects and events beyond the diffraction limit, with the characterizations of single bacterial cells (e.g., protein interactions, antibiotic susceptibility, subnanometer motions),[57,58] and counting of individual gold nanoparticles, with the ability to discriminate between dispersed and aggregated species,[59,60] recently demonstrated.

Halpern et al. report a significant advance in SPRM instrumentation through integration of a near-infrared (NIR) light source and gold-coated knife-edge mirror.[61] Excitation of SPPs with NIR light results in sharper reflectivity curves at lower angles of incidence, yielding greater image contrast changes in response to binding events and allowing for the use of microscope objectives with a lower NA. The knife-edge mirror, used in place of a beam splitter, enabled collection of the full amplitude of collected light and eliminated interference effects from multiple reflections. This instrument setup has been widely applied by Corn and co-workers over the past several years, with applications including studies of DNA hybridization,[61] measurement of melittin uptake into hydrogel nanoparticles,[62] measurement of protein binding to hydrogel nanoparticles,[63] characterization of liposome encapsulation and adsorption,[64] and characterization of protein and polymeric nanoparticles.[65] Additional advances in the technology include computational methods that allow for greater spatial resolution and the ability to resolve binding events that are in close proximity. Yu et al. propose a digital method based on image processing in Fourier space and deconvolution of the complex field, which minimizes the parabolic tails within collected SPR images and yields transverse and longitudinal resolutions close to the limit of diffraction.[66] On the basis of these trends, it is anticipated that further enhancements of

sensitivity and resolving power will likely be dependent on both optical and computational innovations.

SPR techniques have historically been unable to detect small molecules, as their binding to surfaces results in extremely low refractive index changes and, thus, only marginal signals generated. The combined use of SPRM and nano-oscillators, however, provides the means to detect essentially any size molecule with charge in an ultrasensitive manner.[67] The nano-oscillators are comprised of gold nanoparticles tethered to a gold film through a thiolated poly(ethylene glycol) spacer. By applying an oscillating electric field perpendicular to the surface, the nano-oscillators oscillate, which can be individually visualized with high spatial and temporal resolution on an SPR microscope. Binding of charged molecules to these surfaces results in changes in the oscillation frequency, which can be quantified down to 0.18 electron charges independent of size. This method was applied toward real-time monitoring of phosphorylation events[68] and could conceivably be used for screening low molecular weight drugs at the single molecule level.

Fiber Optic Platforms

The discussion on SPR instrumentation has until this point focused on chip-based designs, though SPR sensors may also be constructed from optical fibers that effectively act as waveguiding couplers. The core of an optical fiber is typically made of glass or plastic, which is capable of increasing the momentum of light and allows for a range of incident angles to propagate within the fiber. With the outer sheath removed from a discrete section, a thin plasmonic film may be applied and SPPs may be generated along the outside of the fiber under wavelength (i.e., white light) interrogation (Figure 2D).[69] Alternatively, the fiber can be polished along one side for planar deposition of the plasmonic layer, which was recently demonstrated and characterized using silver.[70] Mathematical modeling suggests that matching the refractive index of the fiber core with the dielectric as closely as possible results in higher sensitivity, in addition to choosing metals possessing lower plasma frequencies.[71] This general setup produces a highly miniaturized design and offers flexibility for sensing in a wide variety of environmental or field situations. However, similar to the chip-based platforms, temperature fluctuations may interfere with measurements, though efficient strategies for mitigation are available on fiber SPR devices. Velázquez-González et al. propose coating the latter half (i.e., closer to the spectrometer) of the exposed gold coating with PDMS, which possesses a much higher index of refraction than is routinely measured in biosensing experiments.[72] This not only produces a second plasmon band for the PDMS coated area but also blocks the gold surface and prevents additional refractive index induced changes for that band, thus producing a signal that is solely responsive to temperature. Similarly, Chen et al. utilize a gold-coated, fused silica capillary filled with water and spliced between two optical fibers.[73] Light may be guided through the capillary walls, generating SPPs over the gold film, and also through the capillary interior, generating Fabry-Perot (FP) interference fringes in the transmission spectra. The FP mode exhibits temperature dependent shifts but is insensitive to refractive index changes, proving that this design can be self-referencing. Multiplexing abilities are also possible with fiber SPR through use of a monochromatic light source and CCD camera for intensity monitoring, with a 3 × 3 protein binding array demonstrated by Liu et al.[74]

Portable Instrumentation

For analyses to be performed on-site within clinical and environmental settings, the availability of portable instrumentation is critical. General requirements for these devices include minimized size, simple operation, and ability to withstand demanding environmental conditions while maintaining desired sensitivity. There are many commercial options available, including NanoSPR (NanoSPR Devices, Chicago, IL, USA), P4SPR (Affinité Instruments, Montreal, Canada), and SPIRIT (Seattle Sensor Systems Corporation, Seattle, WA, USA), which have been used for the detection of a wide variety of targets,[75–77] with use of the P4SPR demonstrated in clinical and field settings.[17,19] Both the NanoSPR and SPIRIT operate under angular interrogation, while the P4SPR operates under wavelength interrogation, and all offer multichannel fluidics for multiplexing capabilities. While SPIRIT carries the advantages of integrated syringe injectors and a contained power source, both the NanoSPR and P4SPR are easily connected to automatic or manual sample injectors, and the P4SPR may be powered via USB through a laptop computer.[19]

In light of the commercialization of SPR technologies, research into instrumentation designed for portability remains active. There have been many mechanical and optical innovations presented over the past couple of years that may inform the design of space efficient devices. For example, Devanarayanan et al. have demonstrated that a rotating mirror, controlling the angle of incidence, and a quadrant photodiode may be used in conjunction with a vertical translation stage holding the prism and sensor chip to generate an angular interrogation device that does not require circular movement of the light source and detector.[78] Michel et al. propose a flexible, wavelength interrogating SPR device that utilizes one fiber optic cable for excitation and data collection.[79] An optical circulator directs incoming and outgoing light through one end of the fiber, while the other end is attached directly to one face of an equilateral prism. The sensor chip and a mirror are placed on the remaining two faces, for SPR detection and redirection of light back into the fiber, respectively. A portable imaging SPR device has also been developed, consisting of a beam splitter, white light source, portable CCD camera, and a grating coupler, which was applied for analysis of mycotoxins in beer.[80] One of the more robust systems noted is the attachment of a custom built SPR instrument to an ocean vessel for the underwater detection of domoic acid.[81] The measurement and spectroscopic components were separately compartmentalized to enhance durability of the device, and computer controlled peristaltic pumps were responsible for directing low volumes of seawater samples to the sensor surface while the vessel was deployed.

Smart phones have become ubiquitous throughout society, and as such, there has been great interest in exploiting their optical components and computational power for the construction of biosensing devices.[82] The integration of a fiber optic SPR sensor based on a flexible silica capillary with a smart phone has been presented by Liu et al., and resolution of the instrument was in the same order of magnitude as a commercial Biosuplar instrument, compared directly within the study (Figure 3).[83] The LED from the phone camera functioned as the light source, which was guided through the fiber and back to the camera itself, functioning as the detector. All instrument operations were performed via a custom written application for the phone. Bremer and Roth developed a similar design, though used

a commercial optical fiber with the cladding removed.[84] Smart phone enabled SPR sensors with grating couplers have also been successfully developed, imaging changes in either reflected wavelength[85] or intensity[86] through the CMOS camera on the phone. The device proposed by Guner et al. utilizes commercial Blu-ray discs as a diffraction grating for the deposited gold film and is capable of multiplexed detection of antibodies in the nanomolar range.[86] Given that smart phones receive hardware and software updates on a consistent basis, the power behind these devices will accordingly increase, providing near limitless opportunities for mobile biosensing laboratories.

MATERIALS FOR PLASMONIC SENSING

In breaking down an SPR instrument, the choice of material for each of its constituent optical components has the potential to influence the sensitivity and overall performance. While many materials are considered standard for SPR instrumentation, a plethora of options exist for manufacturing, with the effects of nonconventional and hybrid materials under active investigation for plasmonic activity. To better appreciate the diversity of materials available in the construction of SPR sensors, applications of both established and newly developed plasmonic signal transducers, prisms, and microscale considerations in chip design are provided in this section.

Plasmonic Materials

Gold is the most commonly used plasmonic material, which benefits from established deposition protocols, surface chemistries, and a general inertness to oxidation under ambient conditions. While silver, copper, and platinum are also involved in discussions around chip design, with intrinsically higher sensitivities than gold, their propensity for oxidation minimizes shelf life and sensor reproducibility. One strategy to mitigate the oxidation issue is to deposit silver and gold in a multilayer fashion, with a final film of gold as the protecting layer.[87] Such a design has been shown to exhibit a higher RI sensitivity than gold alone, though not as high as that of silver alone, though with no deterioration or oxidation of the metal interface exposed to the dielectric. Moreover, these multilayer structures are compatible with both chip and fiber SPR sensors. Once fabricated, gold thin films have been shown to withstand considerable aging times and regeneration cycles, as measured by their analyte binding capacities and analyte binding affinities. From the studies conducted by Steinicke et al., it is important to note that, while the maximum SPR response (R_{max}) provides a good baseline for measuring sensor deterioration, this must be taken into consideration along with measured dissociation (k_d) and association (k_a) rate constants, which may be minimally affected.[88]

Deposition protocols for plasmonic films often vary between facilities, though attempts to standardize evaporation parameters may result in higher quality films and sensors throughout the SPR community. A perspective published by McPeak et al. details key parameters for fabricating high quality gold films, i.e., those with low surface roughness and high uniformity, through thermal evaporation.[89] For the best quality gold films, high vacuums (e.g., 3×10^{-8} Torr) and high deposition rates (e.g., 10 Å s^{-1}) were favored, generating a surface roughness of 0.3 nm (RMS). However, lower vacuums (e.g., 2×10^{-6}

Torr) and low deposition rates (e.g., 0.5 Å s^{-1}) were capable of generating gold films of only marginally lower quality, with a surface roughness of 0.4 nm (RMS). These optimized films exhibited significantly enhanced quality factors, indicative of the proficiency of the metal to perform for plasmonic applications,[90] for SPPs (Q_{SPP}) and localized surface plasmons (Q_{LSP}), in addition to greater SPP propagation lengths over standard literature values. Full optical comparisons of films from all tool parameters, in addition to optimized recipes for silver, copper, and aluminum, were also provided.[89]

Beyond Gold and Silver—Materials scientists have underlined the need for new plasmonic substrates beyond gold and silver due to loss conditions (e.g., interband and Drude losses), oxidation by ambient gases, and high costs of precious metals. Outside the realm of noble metals, a plethora of materials exist that are capable of supporting surface plasmons, from semiconductors to 2D materials such as graphene. Many of these newly developed semiconductor and hybrid metamaterials, in addition to a summary of the shortcomings of conventional plasmonic materials, are thoroughly discussed within a review by Naik et al.[91] As an example, one recent frontrunner material for SPR sensing is aluminum, which is capable of supporting SPPs in the visible, deep UV, and far UV regions of the electromagnetic spectrum.[92–95] Ozaki and co-workers have noted higher refractive index sensitivities using aluminum SPR sensors with UV excitation compared to gold SPR sensors with red excitation in both air and aqueous conditions under angular interrogation.[93,94] Geiss et al. expanded on these studies in a more applied manner through measurement of protein binding using UV SPR.[95] While aluminum forms a native oxide layer at the surface in ambient air, unlike silver, which is more likely to undergo sulfidation, the sensor is amenable to common silane chemistries, which were used for covalent coupling of NTA for protein attachment. A diffraction grating was used in conjunction with wavelength interrogation, which exhibited comparable sensitivities to gold diffraction gratings in the visible region. It is anticipated that the adoption of alternative plasmonic materials, such as aluminum, may overcome many of the shortcomings of conventional plasmonic materials, though further characterizations and method validations will certainly be required.

Alloyed Thin Films—Though nonconventional materials are bringing new capabilities to SPR researchers, one issue that remains is that the optical and mechanical properties of these materials are fixed, with no flexibility in tuning for specific applications. Alloyed materials, on the other hand, provide an opportunity to circumvent this issue, with the alteration of each constituent leading to new properties of the bulk material. One alloy that is perhaps generating the greatest interest is the combination of gold and silver, with intention driven toward preserving the high plasmonic sensitivity of silver with the chemical stability of gold. Gong and Leite have conducted thorough optical characterizations of linear, bimetallic alloyed gradients of gold, silver, and copper in transmission and Kretschmann geometries (Figure 4).[96] These alloys were fabricated through cosputtering of the metals from oppositely angled sources, generating a linear gradient of each metal across a glass surface. For each alloy, higher Q_{SPP}'s were produced throughout the visible and NIR regions at specific compositions, with a 50/50 ratio of gold and silver producing the greatest enhancements compared to other metal mixtures. Such methods could provide a means to produce the highest Q_{SPP} material for the desired application and wavelength range of the

sensor being constructed. In the line of producing uniform structures, the fabrication process for metallic alloys with high compositional homogeneity has undergone investigation by Yin and co-workers for silver/gold nanoparticles.[97,98] The precursor structures were fabricated in a core/shell regime, with gold comprising the core and silver comprising the shell, and high annealing temperatures (>900 °C) were used in conjunction with a protective silica coating to facilitate the diffusion of silver and gold atoms throughout the nanostructures. Energy dispersive X-ray spectroscopic elemental mapping confirmed gold and silver to be evenly distributed throughout the structures, and high plasmonic activity was noted for surface-enhanced Raman spectroscopy. While this annealing technique has not yet been applied for alloyed thin films, the availability of silica deposition methods (e.g., sputter coating, layer-by-layer/calcination, plasma enhanced chemical vapor deposition, etc.) may allow for analogous techniques to be adopted for thin films in the future. Other plasmonic alloys under investigation include silver/aluminum[99] and magnesium/aluminum,[100] both produced by cosputtering, which have undergone optical and morphological characterizations.

Prism Variations

The choice of prism material in SPR sensors is generally made with regards to tuning of the resonance angle, with higher refractive index prisms producing lower resonance angles and vice versa.[101] For imaging, there is also an added benefit in using high refractive index prisms, as lower angles of incidence will lead to less image distortions and stretching of reflected features on the surface. Some of the most commonly used optical glasses are BK7 (n = 1.51), SF2 (n = 1.65), and SF10 (n = 1.72), which each fulfill the resonance matching conditions for SPR and offer accessible ranges of incident angles for 50 nm gold films excited with visible light. When conducting analyses in other wavelength regions, quartz and sapphire prisms have been used for UV-SPR,[93,94] and a fluoride-glass prism has been tested with high sensitivity for NIR-SPR.[102] Beyond tuning of the incident wavelength, however, altering the refractive index of the prism also results in corresponding changes in sensitivity, with lower refractive index prisms producing greater sensor responses.[101] As such, low refractive index prism substrates that are still capable of increasing k_{eff} (i.e., incident light effective wavevector) to match k_{sp} (i.e., SPP wavevector), thus producing higher sensitivities, are under investigation. Early efforts toward this goal utilized low refractive index glass[103] and polymer prisms,[104] each demonstrating enhanced SPR sensitivity over higher refractive index glass prisms, though these materials have yet to catch on with the wider SPR community. Song and co-workers have proposed the use of liquid prisms over solid prisms of glass or plastic.[105,106] In one design, a silver SPR chip was placed within a liquid reservoir that functioned as both the measurement cell and light coupler, with the metallic face of the chip sealed within an inert gas chamber to prevent oxidation and sample interference.[105] In contrast with traditional SPR sensors, increases in the sample refractive index led to decreases in resonance angle, which responded in a negative linear fashion. With the full-width at half-maximum of the reflectivity curve taken into consideration, this sensor displayed a higher figure-of-merit than conventional glass prism sensors. While notable, in that this setup requires a decreased number of optical components, one drawback is that there needs to be a sufficient volume of sample to cover the sensor chip and keep it submerged. Therefore, Lan et al. also developed an aqueous prism model in which the metallic SPR film was enclosed within a traditional flow cell, and the solution that

comprised the liquid prism remained constant. This design also displayed high figures-of-merit and carried the advantages of decreased sample volume and the ability to easily adjust the refractive index of the liquid prism by changing the prism reservoir liquid. Rethinking of standard optical components, as the studies above have done, will be essential to future innovations in instrumentation and performance. With the advent of new fabrication methods, such as three-dimensional printing,[107] an increased variety of materials (e.g., glass, plastics, etc.) and exotic designs will certainly cause the community to rethink how optical and instrumental design are carried out.[108,109]

Microfabricated Features

SPR interactions are often considered with respect to the nanoscale, from molecular binding to electromagnetic coupling, though there are also many microscale factors within material design that can influence sensing performance, particularly for SPR imaging. In regards to sample handling, microfabricated structures can streamline sample deposition protocols, enabling high flexibility in the spatial distribution and sorting of deposited material. Manuel et al. have developed a microwell-printing fabrication strategy so that multiplexed on-chip biosynthesis of fluorescent proteins can be monitored by SPRi.[43] Microwells were laser cut into polyolefin acrylate sealing tape, forming incubation chambers for in vitro coupled transcription/translation, and the protein products could be directly contact printed to a functionalized SPRi chip. Abali et al. were successful in optimizing a similar system for on-chip cell sorting and isolation.[110] Designed for monoclonal antibody selection, the device consists of an SPRi chip functionalized with the intended antigen, and an array of microwells, each seeded with a single cell, placed over the chip. The microwell bases contain a 5 μm pore that allows secreted antibodies to flow through but not the cells themselves. After an incubation cycle, the SPRi chip is analyzed, and the highest producing cells can be identified from the array analysis and then isolated for expansion and high yield antibody production.

Beyond sample handling, microfabricated features have the ability to influence the plasmonic characteristics of the SPRi sensor chip. In SPRi, one recurring issue in measurements is the need to account for background signals outside of the areas of interest. Cheng and co-workers have developed multiple strategies to dampen the evanescent field generated by the underlying glass in Kretschmann geometry, while enhancing the plasmonic field within regions of interest through photolithographic patterning of the deposited metal.[111,112] An elevated gold grid (ca. 100 nm thickness) is fabricated around the regions of interest, which attenuates the evanescent field in the background areas, thus removing all reflections contributing outside of *p*-polarized excitation and increasing the dynamic range of the sensor.[111] Moreover, the electromagnetic fields from SPP propagation within the microwells were found to be enhanced within finite-difference time-domain (FDTD) simulations, and increased refractive index sensitivity over planar gold films and gold island arrays was accordingly noted. It was proposed that the elevated patterns were responsible for reflection of SPPs within the microwells, increasing their intensity in the direction of *p*-polarized light as long as the well diameter remained lower than the SPP propagation length but larger than twice the incident wavelength. Similar effects can be seen if the glass surface is etched with an array pattern before metal deposition, also producing plasmonic

microwells with enhanced contrast and differential resonance over the background.[112] This design has since been utilized for a number of SPRi assays[44,75,113,114] and provides a foothold for further engineering of plasmonic activity through the rational design of microscale features.

INTERFACE DESIGN

Beyond choosing the instrumentation and the plasmonic platform, another important consideration when carrying out SPR analysis is the molecular construction of the sensing interface. Several design considerations must be taken into account depending on the application, including the choice of surface receptor, which will target the analyte of interest, and the method of attaching this receptor to an SPR active material. As SPR requires the use of a metallic surface, most often gold, a common functionalization strategy takes advantage of the dative interaction between a thiol terminal and the metal for direct attachment. In this section, we outline the various surface chemistries that can be used in the construction of an SPR sensor, predominantly focusing on biosensing applications, where surface recognition elements may consist of a number of biological entities, including DNA, antibodies, enzymes, and proteins, with varying chemical linkers utilized.[17,18,41,115]

Self-Assembled Monolayers for SPR

The formation of a self-assembled monolayer (SAM) is one of the most traditional methods of constructing an SPR sensor. Through the spontaneous assembly of sulfhydryl groups onto a gold surface, ordered molecular assemblies can be formed, which often consist of a functional end group and varying constituent molecules that can be tailored to a specific application.[116] Although alkanethiols were the first reported SAMs, there are now many variations in regards to SPR biosensor design, the simplest of which is the use of a thiolated oligonucleotide SAM. Capture DNA strands can be added directly to a gold surface through incubation and self-assembly, with minimized reaction steps, yielding a surface that allows for the detection of various analytes.[41,117] An advantage of thiolated oligonucleotides is that they are relatively simple to obtain, either through the use of an onsite DNA synthesizer or via a number of commercial sources. However, given that there are many other useful receptors that do not have an exposed thiol group or have ones that produce unfavorable receptor surface orientations, traditional SAMs (e.g., alkane- and PEG-thiols) remain popular choices among the community. These consist of a thiol moiety that allows for self-assembly over a gold surface, a spacer molecule, and a functional group that enables coupling chemistries to be carried out for receptor attachment. For example, though there are many options to attach antibodies to a surface,[118] the most common takes advantage of SAMs containing a carboxyl terminal, where the use of carbodiimide coupling chemistry results in the attachment of the antibody through primary amine terminals on its surface. These functional linkers are not restricted to the attachment of antibodies, however, and can be used alongside any capture moiety that has a reactive group against the SAM terminal.[115] Similarly, SAMs are not restricted to intermediate repeating carbon chains; although alkanethiols are still being successfully used for a number of applications,[115,119,120] other functional linkers are being investigated that consist of, for example, polymers and polypeptides.[17,18,121] Mixed self-assembled monolayers, where various functional linkers

are attached to the gold surface in tandem, are also being investigated for their various uses. These have been demonstrated for the control of SAM density on the surface of a sensor,[122] which in turn has been shown to be useful in the tailoring of protein adsorption to the surface.[120,121]

Multidimensional Sensing Interfaces

Beyond self-assembled monolayers, there are a number of other functionalization strategies that can be used to attach receptors to an SPR surface. In fact, one of the most common commercial surface chemistries on the market consists of a matrix of carboxymethylated dextran (CMD), a polymer of carbohydrates terminating in a functional group, which can be activated toward receptor attachment using simple coupling chemistries that are similar to those described for thiolated SAMs. These have been used for both SPR and SPRi analysis,[35,123,124] with evidence provided that CMD performs much better in the attachment of proteins than alkanethiols, likely due to higher availability of binding sites.[124] However, although many have found success with the use of CMD, it is not without disadvantages, with one major consideration being the extended thickness of CMD on the gold sensing surface. Given that the sensing range for SPR is limited, with an average penetration depth of <200 nm,[125] and that sensitivity decreases exponentially with distance from the gold surface, the use of a matrix which can be up to 200 nm thick could drastically hinder the performance of an SPR analysis. Recently Wang et al. compared the use of a commercial CMD chip with a SAM containing a terthiophene derivative.[126] The authors concluded that the use of the terthiophene SAM allowed for better antibody binding, and hence improved assay sensitivity, and that this could in part be attributed to the sensing interface being closer to the gold surface.

An emerging platform that allows for the simple attachment of biomolecules is the use of graphene and graphene oxide sheets in combination with SPR. Graphene oxide consists of sp^2- and sp^3-hybridized carbon atoms that allow for biomolecular interactions to occur through π-stacking, in addition to many attractive functional groups (e.g., carboxyl, hydroxyl, etc.) that are capable of further derivatization.[127,128] Stebunov et al. have investigated an airbrushing method for depositing graphene oxide layers onto gold SPR surfaces and compared the sensor performance to pristine graphene and a commercial CMD matrix.[127] The graphene oxide layer exhibited better performance in the attachment of streptavidin than both the CMD and graphene coated chips, with the additional advantage of controllable thickness of the sensing layer, an issue previously discussed for CMD surfaces. While this example utilized the attachment of a receptor though π-stacking interactions, Chiu et al. investigated the use of carboxylated graphene oxide composites as biosensing interfaces for SPR, which were formed over a SAM of cystamine.[128] It was concluded that the carboxylated graphene exhibited enhanced SPR sensitivity over unmodified graphene oxide, demonstrating that this surface can be easily tailored to suit a variety of analytical requirements. However, while graphene oxide allows for simple and varied methods of biomolecular attachment to SPR surfaces, its synthesis and attachment to gold often require multiple steps and increased labor, thus reducing efficiency in interface design, a trade-off that should be taken into account during assay development.

Ease of surface preparation is certainly an important consideration during the design of a sensor, and one method that allows for minimized effort in the modification step is the use of polydopamine. This biologically inspired interface is created by the polymerization of dopamine into thin films across a variety of organic and inorganic surfaces, which occurs spontaneously in slightly basic aqueous solutions.[129,130] Also under these basic conditions, *o*-quinones present in dopamine and polydopamine may form covalent bonds with amine- or thiol-terminated biomolecules via Michael addition or Schiff base reactions[129,131] and as such represent an exciting new surface chemistry for use in SPR. Wood et al. demonstrated the polymerization of dopamine onto a gold microarray surface in real-time using SPRi: by simply injecting a buffered solution of dopamine over the gold, the thickness of the polydopamine layer could be carefully controlled by altering the deposition time. Aside from the simplicity of preparation and controlled layer thickness, the authors also demonstrated the ease of biomolecular attachment by conjugating amine terminated DNA directly to the polydopamine surface, with no additional reagents required.[130] Toma and Tawa additionally demonstrated the attachment of antibodies to a polydopamine thin film created under the same mild reaction conditions and in the absence of any coupling agents.[132] They were able to monitor the binding of a capture antibody to the surface in real-time and noted that these immunoreceptors tightly bound to the biopolymer within a rapid time frame. Similarly, Shi et al. successfully utilized polydopamine for the attachment of an antibody onto a gold film, although for use in an optical fiber SPR setup.[131] The authors compared the attachment of a human-IgG antibody onto a polydopamine surface to its conjugation onto an alkanethiol via traditional coupling schemes. Antibody immobilization onto the polydopamine was shown to be more effective, and it was suggested that this is likely due to increased binding sites, less steric hindrance, and elimination of hydrolysis issues associated with EDC/NHS coupling chemistry. As such, polydopamine represents a very interesting surface chemistry for use in SPR, since the thickness of the layer can be carefully controlled, and biomolecules can be easily attached with minimal reagents and under mild conditions, with reports demonstrating that this attachment chemistry is more efficient in comparison to traditional conjugation methods. While all of the above examples represent novel surface chemistries that have numerous advantages as part of the toolbox available to SPR researchers, considerations must also go beyond ease and success of attachment, with designs converging on a material that is actually functional for targeted and specific analytical applications.

Antifouling Surface Chemistries

Though there are numerous options for attaching a receptor to an SPR surface, the specific application must be considered when designing an appropriate surface chemistry. Regardless of the specific area of analytical chemistry that SPR will be used for, be it in clinical diagnostics, forensic science, food science, or various other applications, it is likely that the analyte of interest will be contained in some sort of complex matrix. Taking clinical diagnostics as an example, biomarkers of interest are often found circulating in the bloodstream, thereby leading human blood serum and plasma to represent some of the most common biofluids analyzed.[7] Unfortunately, these protein abundant matrices represent one of the most difficult samples for SPR, given the propensity of functionalized and unfunctionalized gold chips to nonspecifically adsorb biomolecules. Since SPR is a

refractive index-based method of analysis, it is often difficult to distinguish nonspecific signals from those that are analytetriggered. Unsurprisingly, there are numerous efforts being undertaken to mitigate this issue, with the majority of solutions revolving around interface design.

A number of the surface chemistries previously discussed in this section have been used or adapted for use in the analysis of complex matrices. Indeed, the commercial CMD surface is marketed as an antifouling interface, although it's use in the analysis of complex matrices is limited, often requiring dilution of the sample in buffer prior to analysis, which restricts the capabilities of the sensor.[7,133] The use of graphene and graphene oxide coated SPR sensor chips is an excellent example of how the surface chemistry design must take into account both biomolecule attachment and application, since the ease of attachment for this surface also results in extremely high levels of nonspecific binding when carrying out analyses in complex matrices due to the surface not being able to discriminate between target and nontarget biomolecules. However, He et al. used this nonspecific affinity for material in human serum to their advantage, incorporating graphene as part of the surface blocking procedure in order to develop a SPR chip capable of carrying out analysis directly in human serum.[134] He and co-workers were also successful in taking advantage of reactive groups to design a low fouling hyaluronic acid surface through coupling of dopamine to hyaluronic acid prior to gold surface attachment, ultimately providing an example of how this type of surface chemistry could undergo a simple modification to allow for its use alongside complex matrices.[133,135] Dang et al. similarly investigated the ability to improve the biofouling properties of polydopamine using simple chemical modifications, and by grafting a phosphocholine copolymer to the polydopamine surface, the authors were able to drastically reduce the amount of nonspecific binding from a variety of biomolecules.[136]

Polymers represent one of the most extensively reported classes of antifouling materials, with their hydrophilic and/or zwitterionic natures contributing to reductions in nonspecific protein adsorption.[121,137] Poly(ethylene glycol) (PEG) is an example of a common polymer which can suppress protein adsorption via its hydrophilic nature and can easily be used alongside SPR if PEG is terminated with a thiol. A variety of exposed functional groups can also be derivatized with PEG for receptor attachment. Hybrid attachment chemistries incorporating PEG have been developed, with Koelsch and co-workers reporting the attachment of these hydrophilic polymers to a polydopamine surface, creating dense polymer brushes which exhibit excellent antifouling properties.[138] Polymer brushes themselves represent a class of antifouling materials, where closely packed polymer molecules adopt a stretched confirmation and are commonly created by various surface initiated and controlled polymerization methods.[139,140] Polymer brushes can be constructed from many repeating molecular units, though some common examples include the use of oligo(ethylene)-glycol (OEG), hydroxyl containing methacrylate monomers, and zwitterionic polymers.[121,139,141]

Recent trends in antifouling materials for biosensing have seen a shift toward the use of zwitterionic molecules due to their superior ability to resist protein adsorption. These materials possess adjacent and oppositely charge residues, retaining a localized net neutral charge, and are thought to repel protein absorption via the electrostatic creation of a

hydration layer.[121,141] Antifouling zwitterionic materials often reported for sensing include poly(carboxybetaines),[141–144] polypeptides,[145–147] and phosphocholines.[148–150] Ye et al. recently compared the anti-fouling capabilities of two polypeptides, one of which was an amphiphilic, nonionic heptapeptide and the other was zwitterionic in nature.[146] SPR sensor surfaces were created by the self-assembly of these polypeptides onto a gold surface via interaction with N-terminal cysteine residues and were exposed to both individual proteins and complex media. It was demonstrated that, although the amphiphilic peptide SAM exhibited good antifouling properties toward single proteins, the zwitterionic peptide had an improved performance toward both single proteins and natural protein matrices, which was attributed to an increased and stable hydration layer surrounding the zwitterionic peptide.

Although their ability to resist proteins is greater than traditional SAMs and PEG-based coatings, the zwitterionic surface must remain amenable to receptor functionalization for sensing applications without sacrificing the antifouling properties.[139] This is a particular problem in the use of certain zwitterionic brushes, whereby activation of the functional groups toward conjugation drastically reduces their antifouling properties.[151] Homola and co-workers recently carried out an in-depth study of various carboxyl-functionalized coatings, investigating the effect of functionalization on the antifouling characteristics.[151] Carboxybetaine and copolymer brushes were the main foci, which were compared to conventional carboxylated OEG SAMs for their ability to undergo amide coupling and remain resistant to nonspecific protein adsorption within blood plasma. In tailoring the carboxybetaine concentration within the copolymer brushes, as well as deactivating the coupling procedure with glycine, excellent antifouling properties were demonstrated, which exceeded the results obtained from the homopolymers and conventional SAM surfaces. As future interfaces are developed, researchers must be willing to thoroughly investigate the antifouling characteristics before and after biomolecule derivatization, which may substantially change.

The specific matrix in which biosensing will be conducted may have a substantial impact on the antifouling performance of the sensing interface, and although a large portion focus on the nonspecific absorption from human blood serum and plasma, there are a variety of other matrices, even within the clinical diagnostic field, that could potentially be useful for sensing. Aubé et al. recently reported on the use of an ionic liquid self-assembled monolayer as an antifouling surface for analysis in crude cell lysate.[20] The authors began by discussing the nature of cell lysate in comparison to blood-based matrices, such as serum and plasma, and noted that antifouling surfaces designed for the latter are not successful in the analysis of cell lysate[20,145] and that reports of successful sensor surfaces for this type of matrix are scarce, regardless of the fact that many interesting diagnostic biomarkers are present within this biological fluid and in high abundance. The antifouling properties of various ionic liquid preparations against cell lysate were compared to those of common antifouling surface chemistries, including polypeptides and PEG monolayers, and the ionic liquids were demonstrated to be far superior in performance.

The field of antifouling coatings is extensive, with the options for SPR interfaces ever increasing. For example, while clinical diagnostics have been the primary highlight, less explored matrices have included food and environmental samples.[9,19,152–154] Although

food-based samples represent an extremely complex matrix, there are very few reports of ultralow fouling surfaces specifically designed for this purpose.[152–154] Vaisocherová-Lisalová et al. propose the use of a rationally designed copolymer brush that exhibited high fouling resistance against various food matrices, and the authors showed that this resistance remained consistent even after functionalization with a biorecognition element.[152] An increased supply of functional materials will be required for effective sensor design that combines tailored antifouling activity with the ability to efficiently attach biorecognition elements for the sensitive detection of target analytes.

Biomimetic Interfaces

The notion of taking lessons from nature while designing a biosensor surface has great advantages in the field, as biological interactions can potentially be studied on a platform more representative of a native environment. Biomimetic surfaces were introduced briefly in the previous section, where the use of polydopamine, an interface inspired by mussel adhesion, was used in the construction of a simple and effective surface chemistry with attractive properties for SPR analysis. The use of zwitterionic antifouling surfaces consisting of phosphocholines is another example of how naturally occurring chemistries can successfully be used in the design of an SPR sensor. An example of such a biomimetic system exists in the use of supported lipid bilayers, which are simplified systems that model the cellular membrane, and the constituents of which can easily be altered to allow for specific biomolecular assays to be carried out at the lipid membrane interface.[155,156] There are many ways to construct supported lipid bilayers,[156] including vesicle fusion over a hydrated surface[44,157] or attachment to an underlying surface chemistry,[158] which allows for surface-based analyses, such as SPR, to be conducted.[76,156] Cheng and co-workers developed a benchtop method for creating nanoscale layers of glass on gold SPR substrates via a layer-by-layer deposition and calcination (LbL/calcination) approach, which produced hydrophilic surfaces that were capable of promoting vesicle fusion toward a fluid supported lipid bilayer on an SPR chip.[159–161] These nanoglassified gold sensor surfaces were used in the analysis of membrane bound proteins by SPR[157] and SPRi,[162] with Hinman et al. recently utilizing the methods to study the formation of hybrid bilayer interfaces consisting of phosphocholine and synthetic amphiphilic dendrimers.[76] Supported lipid bilayers on nanoglassified SPR chips have been extensively applied for the investigation of water-soluble deep cavitands, which self-incorporate into the bilayer, forming a pocket capable of hosting a wide variety of proteins and functionalized molecules.[114,163–165] Perez et al. demonstrated the use of these cavitands embedded within a supported lipid membrane for site-specific polymer growth at this biomimetic interface, enabling the attachment of nonadherent cells and proteins.[163] One of the disadvantages associated with this interface is the inherent instability when exposed to air, limiting their use in the individually addressable arrays. Hinman et al. have proposed the use of trehalose vitrified phospholipid vesicles, which can be applied in array format to SPR sensors coated with silica using plasma-enhanced chemical vapor deposition (Figure 5).[44] The trehalose functions to preserve vesicle morphology during desiccation, allowing arrays to be dried and stored under ambient conditions before rehydration. Vesicle fusion occurs immediately when aqueous conditions are reestablished within an SPR(i) flow cell environment, and full functionality with regards to monitoring interactions with membrane bound receptors was demonstrated. Altogether,

the simplicity of surface modification, compositional control, and amenability toward array screening make the combination of supported lipid bilayers and SPR an extremely exciting example of how biomimetic interfaces can be successfully utilized.

SIGNAL ENHANCEMENT

Surface plasmon resonance is an ideal detection strategy when the analyte of interest causes a significant change in refractive index; however, when analyzing smaller molecular weight analytes or those that are present in low quantities, enhancement mechanisms can be employed to boost the signal achieved upon biomolecular binding events. For example, SPR-based biosensors commonly consist of a sandwich immunoassay, whereby a recognition antibody is bound to the sensor surface, and following antigen binding, the signal is further increased through the addition of a detection antibody. Plasmonic enhancement using metallic nanoparticles in place of, or in combination with, a detection antibody is also practiced. The topic of enhancement in SPR has itself been extensively reviewed, and expansive accounts of this area of research can be found elsewhere;[3,4,8,166,167] in this section, we aim to cover the most recent developments in the field, not only pertaining to plasmonic enhancement but also looking at novel mechanisms of increasing the signal achieved using SPR analysis.

Plasmonic Nanoparticles

As previously stated, one of the most common methods of signal enhancement in SPR is through the use of plasmonic nanoparticles, of which gold has been the main focus. In its simplest form, binding of these nanoparticles provides a significantly increased refractive index near the sensor surface, and given that SPR is a refractive index-based technique, accordingly increased signals are obtained. However, additional enhancement is possible from the plasmonic coupling that may occur between the surface plasmon polaritons (SPPs) propagating across the SPR chip and the localized surface plasmons (LSPs) oscillating around the nanoparticles. By carefully tuning the plasmonic properties of the gold nanoparticles (e.g., absorbance wavelengths, electromagnetic field intensities, etc.), the sensitivity of the overall sensor can be improved.[4,167] Gold nanoparticles have been successfully utilized within a number of biosensing applications.[6,75,120,157,168–170] For example, Wu et al. recently reported on the use of gold nanoparticle enhanced SPR detection of C-reactive protein (CRP) through the use of an aptamer–antibody sandwich assay.[168] In this sensor design, an aptamer specific to this inflammatory biomarker was immobilized on an SPR active gold surface, taking advantage of the simple attachment chemistry afforded by the use of thiolated DNA. The signals obtained from the binding of CRP were compared to those of a sequential antibody enhancement and a sequential antibody–gold nanoparticle conjugate enhancement. It was concluded that the gold nanoparticle enhanced aptamer–antibody sandwich assay provided the best results with the largest measurement range and lowest detection limit and was applied to the detection of CRP in diluted human serum. While this assay format took advantage of antibody-functionalized gold nanoparticles, Li et al. utilized streptavidin-functionalized gold nanoparticles for enhanced SPR signals in the detection of carcinoembryonic antigen (CEA).[169] In this assay format, a commercial carboxymethylated dextran coated chip was used to attach the recognition antibody, and

after the addition of CEA, a biotinylated antibody was introduced followed by the streptavidin coated gold nanoparticles, which increased the signal significantly in comparison to a direct assay approach. These examples demonstrate that gold nanoparticle enhancement can be used alongside a variety of surface chemistries depending on the final application, similar to the attachment of recognition elements to a thin metallic film. With the ultimate aim of creating stable and functional nanoparticles for sensing applications, the chemistries involved in creating a bioconjugated gold nanoparticle can take advantage of many of the strategies discussed previously, from traditional methods involving carboxylated alkanethiols to novel methods consisting of zwitterionic compounds.[75,171,172] Hinman et al. recently reported on the use of functional DNA linkers and diluents to conjugate proteins and small molecules to gold nanoparticles, a strategy which provided vastly improved colloidal stability over other commonly used methods of conjugation.[75] The authors demonstrated the stability of these nanoparticles against high ionic strength solutions, common fouling matrices, and lyophilization. Furthermore, these ultra-stable conjugates were applied as enhancement agents within SPR and SPRi assays for the detection of cholera toxin at a lipid bilayer interface with excellent reproducibility.

While the majority of these examples utilize the enhancement capabilities of spherical gold nanoparticles, gold nanoparticles can come in a variety of shapes and sizes, which will impact both the extent of refractive index change they can affect and their plasmonic properties.[173] Kim and Lee recently reported on a gold nanostar enhanced aptamer–antibody detection strategy for the analysis of an antibiotic, which as a small molecule analyte, would be difficult to analyze using a direct SPR assay (Figure 6).[115] Using a surface-based aptamer probe and gold nanostars conjugated with a detection antibody via an alkanethiol linker, attomolar concentrations of the target antibiotic were able to be analyzed, and the authors attributed this sensitivity to both the nanoparticle mass and significant overlap between the SPR excitation wavelength and the absorbance of the nanostars resulting from their unique plasmonic characteristics. Lee and co-workers have also investigated the use of gold nanocubes,[174] comparing their use to those of gold nanorods and quasi-spherical gold nanoparticles.[173] In a novel approach to enhancement, capabilities of dual nanoparticle SPR analysis for the detection of thrombin at subattomolar concentrations were investigated.[175] The authors loaded gold nanorods and quasi-spherical gold nanoparticles in varying configurations to determine the best possible enhancement for a biosensor utilizing a surface bound antibody as the primary recognition element, and an aptamer sequence, conjugated to one of the gold particles for enhancement. These methods were able to push the boundaries of sensitivity beyond that which could be obtained for enhancement with a single nanoparticle and open the door for future considerations of mixed nanoparticle enhancement systems with varying geometries and plasmonic characteristics.

Although other plasmonic nanoparticles are available,[167] gold nanoparticles remain at the forefront of SPR enhancement mechanisms, most likely due to their simple synthesis and conjugation using well documented procedures. However, other nanoparticles have recently been employed to a great effect, without the requirement of a localized surface plasmon being present.

Non-Plasmonic Enhancement

Iron oxide nanoparticles are commonly reported enhancement agents,[8,176,177] whereby in the absence of a localized surface plasmon, these nanoparticles solely enhance the signal via increased high refractive index.[8] Given that these nanoparticles are magnetic in nature, issues associated with separation and concentration at a sensor surface can be overcome without the need for expensive or sophisticated equipment. Reiner et al. recently employed magnetic nanoparticles within a grating coupled SPR biosensor for the analysis of extracellular vesicles, which are often difficult to analyze due to their small size and diffusion limited binding kinetics to the sensor surface.[176] Streptavidin coated magnetic nanoparticles were able to bind to the extracellular vesicles via a biotinylated lipid-binding handle in solution and were concentrated at an antibody coated SPR surface using an external magnetic field gradient. Enhanced signals were attributed to the increased binding rate and increased mass on the surface, and it was noted that, by applying the external magnetic field, limits of detection could be achieved that were not possible with direct SPR analysis or nanoparticle enhanced analysis in the absence of a magnetic field. Similar to gold nanoparticles, iron oxide nanoparticles can be conjugated with biorecognition elements through developed protocols, with Liu et al. recently utilizing antibody coated magnetic nanoparticles that were specific for surface receptors on the bacterium *Salmonella enteritidis*.[177] These antibody coated iron oxide nanoparticles were able to recognize and separate the bacteria from a bulk solution through use of a magnetic field, prior to being introduced to the SPR chip. The signal was greatly enhanced compared to direct detection of *S. enteritidis* as a result of enrichment and signal amplification by the magnetic nanoparticles. Although iron oxide nanoparticles alone have been successfully used alongside SPR analysis, the addition of a plasmonic element has been reported by coating the particles with a nanoscale layer of gold, creating core–shell magnetic nanoparticles for enhanced SPR.[178,179] These enhancing agents take advantage of all the properties inherent in magnetic nanoparticles, while adding the potential for plasmon coupling and gold surface chemistries and, as such, can be an extremely versatile tool in enhanced SPR.

Liposomes have also been employed to a great effect as enhancing agents for SPR analysis. Fenzl et al. took advantage of the hydrophilic cavity within liposome vesicles to encapsulate high refractive index solutions that enable tunable refractive index changes near an SPR interface (Figure 7).[180] The authors were able to determine that increasing the refractive index of the encapsulated solution increased the SPR signal generated and that the liposomes could easily be tailored by simply changing the encapsulant to match the dynamic range and sensitivity required. In an adjacent study, Fenzl et al. investigated the nonspecific binding between anionic liposomes and varying surface modification strategies to alter charge and hydrophilicity.[181] Nonspecific binding of an enhancing tag to an SPR sensor surface is a common problem, and the authors noted that the constituents of the lipid-bilayer shell could easily be modified to reduce the nonspecific binding to common surface chemistries. The ability of liposomes to provide a high signal in response to specific surface interactions, while keeping nonspecific binding to a minimum, makes them an upcoming tool for refractive index-based signal enhancement.

Although all of the examples so far have employed nanoparticles, there are other mechanisms of enhancement, including those taken from native biological process, such as enzymatic reactions. One of the most well-known cases of enzymatic signal generation biosensing is the enzyme-linked immunosorbent assay (ELISA), in which a peroxidase enzyme is employed to catalyze an electron transfer reaction resulting in a concentration dependent color change in the presence of a specific target. A similar reaction has also been employed for enhanced SPR whereby, instead of a color change, peroxidase is able to catalyze the formation of a precipitate onto a sensor surface, increasing the signal through increased refractive index and effective mass at the surface.[123,182] Nucleic acid amplification methods have also been used for signal enhancement,[183,184] with examples recently transitioning from enzyme-catalyzed DNA polymerization to DNA self-assembly (e.g., hybridization chain reaction, HCR), as these newer methods do not require the use of additional enzymatic reagents, which can be temperature sensitive and unstable.[183] Ding et al. used a nonlinear HCR to enhance the SPR signals for target DNA sequences and a small molecule.[183] During the nonlinear HCR process, high molecular weight DNA assemblies were constructed in a branched fashion to enhance the signal obtained. In a testament to the versatility of nanoparticles, these nucleic acid amplification strategies have also been combined with nanoparticle localization for use in ultra-sensitive SPR analysis.[185–188] In an example of such a sensing strategy, Wang et al. enhanced the signal via the introduction of DNA conjugated gold nanoparticles which specifically bound to an SPR sensor in the presence of microRNA.[186] These conjugated nanoparticles acted as both a primary enhancement mechanism via plasmonic coupling and as a platform for secondary enhancement via the self-assembly of a high molecular weight DNA coating.

Surface-Based Enhancement

While the majority of SPR interfaces take advantage of the propagating surface plasmons obtained from the use of a thin metallic film, recent advantages in various forms of lithography have allowed nanoscale features to be constructed into SPR active features that exhibit their own enhancement capabilities. Taking periodic nanohole arrays as an example, localized surface plasmons dominate at the feature edge and SPPs propagate over larger areas. Extraordinary optical transmission (EOT) is noted on such substrates, for which the detection and optical geometry will not be the focus here but have been discussed in detail elsewhere.[1,189–194] These nanohole surfaces have also exhibited great utility for SPR in the Kretschmann configuration, allowing for surface-based enhancement of sensitivity.[194] Outside of nanolithographic methods for surface patterning, nanoparticles can be deposited from a bulk suspension and used in combination with a thin metallic film, as Wu et al. have recently demonstrated using hollow gold nanospheres.[195] By coating the gold surface with these nanoparticles, followed by formation of a polydopamine layer, a platform for convenient antibody attachment was created. Due to the high antibody loading capabilities of this interface and the unique optical properties of the hollow gold nanospheres, the authors were able to obtain greatly enhanced SPR signals from a standard sandwich assay design compared to traditional surfaces.

Another approach to patterning a surface and one of the more rapidly growing areas of surface-based enhancement is the use of graphene and its derivatives over gold, and although

graphene was discussed previously due to its ability to act as a platform for attaching recognition elements to a sensor surface, it has also been shown to contribute to the overall SPR signal obtained.[196,197] Singh et al. deposited a single graphene sheet onto a gold metallic film using chemical vapor deposition, and this interface, which was largely continuous and defect free, was used in an immunoassay (Figure 8).[196] The authors investigated different methods of attaching biorecognition elements to the graphene surface using various surface modifications and noted enhanced SPR signals that they attributed to the optical properties of graphene, notably its tunable absorption and its ability to change the propagation constant of the SPP, hence increasing sensitivity to the refractive index. Graphene modified gold surfaces have also been used in combination with secondary enhancement mechanisms[198,199] or used themselves as a secondary enhancement agent.[200] In the latter case, the versatility of polydopamine was further investigated and Hu et al. synthesized a polydopamine-reduced graphene oxide (rGO) composite prior to attachment of an antibody.[200] This construct was then used to form an immunocomplex within an SPRi setup, whereby polydopmaine also acted as a site for the growth of gold nanoparticles, further increasing the final signal. This dual method of signal enhancement, from both rGO and gold nanoparticles, allowed for low limits of detection and a broad dynamic range, demonstrating that a number of strategies can be combined for greater effect.

HYPHENATED ANALYSIS

As is the case in nearly any analytical technique, restriction to one method alone typically results in an incomplete understanding of the system under investigation due to inherent limitations in all instrumentation. In the case of SPR, while creating selective and reproducible sensing surfaces is imperative toward extracting accurate quantitative information, it is often not possible to unambiguously identify ligands attached to the surface, as any bound molecule, target or nontarget, may induce a measurable signal. The addition of complementary analytical methods that are capable of molecular identification, or that may be enhanced through plasmonic mechanisms, is therefore advantageous. Many of these methods can be performed in situ and, in some cases, within an SPR device containing integrated components for multidimensional analysis. Throughout the past few years, there has been much focus on the integration of SPR with mass spectrometry, fluorescence, and electrochemistry.

Mass Spectrometry

Mass spectrometry (MS), which provides measurements based on the charge and molecular weight of ionized chemical species, is one tool that has been shown to substantially increase the informational power of biosensing materials. While comparatively costly and not capable of measuring biological interactions in real-time, mass spectrometric methods have shown great utility toward resolving complex biological structures and are capable of sophisticated tasks such as protein and nucleic acid sequencing. With regard to SPR coupling, a number of methods are possible, which have been divided into two groups by Stigter et al.: (1) SPR is used as an elution method, with the target removed from the sensor chip prior to MS analysis, or (2) MS analysis is performed directly on the gold film.[201]

There have recently only been a few studies using SPR as an elution method prior to MS,[202,203] along with improved instrumental developments for integrated ionization. Liu and co-workers have developed an interface between SPR and direct analysis in real time (DART) MS, in which the outlet fluidics from an SPR sample chamber were connected to a nebulizer at a DART ion source.[204] This technique benefits from being able to take place in ambient conditions, not requiring a high voltage applied to the sample or vacuum conditions and was applied toward monitoring of model small molecules in salt-containing buffers by SPR and DART-MS. Impressively, the presence of physiological salt concentrations did not interfere with MS analysis, which is normally the case with electrospray ionization (ESI) methods that often require a desalting step. A similar ionization method to DART, dielectric barrier discharge ionization (DBDI), which also takes place in ambient conditions though uses a plasma jet, was later developed by the same research group for SPR coupling.[205] This technique was also successfully tested for four model compounds and was found to be more salt-tolerant than the previously established SPR-DART-MS method.

Matrix-assisted laser desorption/ionization mass spectrometry (MALDI-MS) has remained a popular MS method for SPR coupling, as it is surface-based and the only preparations that need to take place after SPR analysis are the addition of an organic matrix to the SPR surface, followed by insertion of the SPR sensor chip into an appropriately configured mass spectrometer. SPR-MALDI-MS falls into the second group of SPR-MS methods proposed by Stigter et al.,[201] with ionization taking place directly on the sensor surface, saving preparation time and materials costs. Masson and co-workers have applied SPR-MALDI-MS toward the identification of biomolecules adsorbed from crude fluids and tissues.[119,206] Within the study by Forest et al., SPRi was used to quantify the amount of adsorbed protein from mouse kidney tissue on various functionalized gold surfaces, while MALDI imaging was used to spatially resolve the identity of multiple proteins directly from the SPRi chip (Figure 9).[119] Anders et al. have also applied SPRi-MALDI-MS, though in an array format, toward the characterization and identification of a kinase from cell lysate.[207] The authors indicated that careful optimizations were required for on-chip proteolytic digest conditions and organic matrix application. The methods reported by Yang and Cheng, utilizing self-assembled monolayers and affinity-based capture, may provide a means to achieve more consistent measurements in SPR-MALDI-MS analysis.[208] An exciting advance, however, lies in matrix-free ionization regimes, completely eliminating the need for optimization of matrix deposition and cocrystallization conditions. Though several surface-assisted laser desorption/ionization platforms have been coupled with plasmonic interrogation methods,[209,210] none have yet been interfaced with SPR.

Biochip Spray MS, developed by Joshi et al., represents a highly simplified way of coupling SPR to MS and may be the most amenable for widespread adoption.[211] The setup uses a modified desorption electrospray ionization (DESI) source, with the SPR chip mounted in front using an alligator clip connected to the DESI high voltage power supply. After an organic solvent (e.g., methanol) is applied to the chip and the high voltage is applied, mass spectra can be acquired from the chip surface under ambient conditions. Biochip Spray was applied for analysis of dioxynivalenol both in a purified form and spiked into a beer sample, with time-dependent monitoring of ion chromatograms possible. While still requiring removal of the SPR chip and drying prior to MS analysis, sample handling was minimized in

comparison to SPR-MALDI-MS as no external reagents beyond an organic solvent were required. Furthermore, SPRi on a 2 × 2 array was proposed to envision the possibility of multiplexed detection in conjunction with Biochip Spray. The integration of automated chip handling and spatially targeted voltage applications may eventually render this method as capable as MALDI in regards to throughput, providing another tool for coupled SPR-MS analysis.

Fluorescence

The hyphenation of fluorescence and SPR may not be immediately intuitive, as both are optical spectroscopies, with one requiring labeling of a reporter for detection and the other one not requiring any labeling unless sensitivity needs to be enhanced. However, Breault-Turcot et al. have made a strong case for the coupling of these sensing modalities on the basis that they are susceptible to different interferences, thus providing positive controls against each other, and that they may function toward extending the dynamic range of the overall assay being developed, provided that the dynamic ranges of the respective techniques partially overlap.[212] As a proof-of-concept, an instrument capable of simultaneous SPR and fluorescence measurements was developed and applied for detection of prostate specific antigen (PSA) via an enzyme-linked immunosorbent assay (ELISA). Hyphenated measurements of PSA in the clinical range could be achieved with a 4 orders of magnitude dynamic range, exceeding that of conventional ELISAs, which are typically 2 orders of magnitude.[212] Alternatively, simultaneous SPR and fluorescence microscopy can be performed, as recently demonstrated by Liu et al.[213] A sensor surface functionalized with folic acid was used, and various cell lines were investigated for their affinity based on differential folic acid receptor expressions. SPR was used for quantitation of binding, while fluorescence microscopy was used to investigate the spatial distribution of attached cells. This technique may be beneficial for specific cases in which SPRi does not possess the necessary sensitivity to detect and spatially resolve certain interactions, such as small molecule binding, or large molecule interactions that only cause minute variations in refractive index over water or buffer.

Surface plasmon fluorescence spectroscopy (SPFS) is a technique that leverages the evanescent field from SPP propagation to enhance emission from fluorophores placed a specific distance away from the gold film (e.g., 15–20 nm). Below this distance, nonradiative energy transfer to the metal occurs, resulting in attenuated or quenched signal, while above this distance, the evanescent surface plasmon field continues to decay, resulting in correspondingly lower enhancement factors.[214] Sergelen et al. recently used this system for adenosine and ATP detection using conformation-switching hairpin aptamers, end-labeled with a fluorophore.[215] In the “off” state of the aptamer, the fluorophore end orients toward the gold surface, bringing the reporter within the attenuation distance of the metal. In response to analyte binding, the hairpin opens, tethering the fluorophore within the SPFS enhancement region. Orientation of the aptamer and fluorophore, spacer length, and incident angle for SPP excitation all required optimization to achieve 23-fold enhancement of detected sensor signal. A split aptamer design, with separated oligonucleotides containing different recognition elements for the same molecule, can also be utilized for detection of low affinity targets under this scheme.[216] In addition to Kretschmann-based setups, grating

couplers can be used for SPFS, for which the grain size, surface roughness, and height profile of the metal can each influence the magnitude of fluorescence enhancement.[217]

Electrochemistry

Electrochemical SPR (EC-SPR) can be adapted from nearly any conventional SPR setup, as EC-SPR utilizes the gold SPR chip as the working electrode, with separate counter and reference electrodes placed in either a reference chamber filled with buffer or the measurement channel itself. This setup is compatible with a range of SPR techniques, including fiber SPR as demonstrated by Yuan et al. using a gold-coated, grating-imprinted single mode fiber that did not require removal of the cladding.[218] Such combinations allow for the isolated study of surface localized electrochemical reactions originating from bound biomolecules and films, as SPR is affected by the local charge, for which changes can produce a measurable optical and electrochemical signal. Laurinavichyute et al. have proposed that the adsorption of chloride, which is present in the majority of biological samples, is the main mechanism influencing the potential of the gold film, thus affecting the SPR response at rest and when potential is applied.[219] EC-SPR has been broadly applied for understanding the electrochemical properties of various interfaces, including real-time monitoring of electron transfer during surface-initiated atom transfer radical polymerization (SI-ATRP), and characterization of the effect of methylene blue density on SPR response as the molecule is undergoing oxidation/reduction.[220] The technique has also been successful in characterizing biological redox reactions, such as the turnover of cytochrome c between its oxidized and reduced forms.[221] Tao and co-workers were impressively able to monitor this reaction using plasmonic electrochemical microscopy (P-ECM, similar to SPRM)[222] with nanosecond temporal resolution,[223] revealing conformational changes in cytochrome c to take place over time scales ranging from microseconds to milliseconds (Figure 10).[224]

OUTLOOK

SPR has undertaken a dramatic growth in the past several years, not only in the amount of use and attention it has garnered but also in the variety of ways it has been applied. Owing to innovations in engineering, optics, and data processing, SPR may now be conducted within a multitude of environments in which the goals may substantially vary. Many scientists, from hospital technicians to nanoscale imaging specialists, can find a use for SPR, with a suite of available instrumentation that may cater to their needs. The introduction of portable instrumentation from multiple suppliers will assist in bringing the technique to an increased number of environments, and as the technical details improve, including the ability to account for extreme climate and charge transfer conditions, it is expected that the quality of measurements will as well. However, in designing any sensor, the instrumentation will only get the user so far, and the design of novel sensing interfaces is often equally as important as the quality of the instrument itself. There are many interfacial facets that must be taken into account when designing a surface amenable to successful analysis by SPR, including the choice of recognition element, the chemistry by which it will be functionalized to the sensor surface, and considerations pertaining to the matrix in which it will be analyzed. New interfaces, including bioinspired polymers, 2D materials such as graphene, and those designed to mimic the cell membrane, are under aggressive development with demonstrated

successes in the achievement of these goals. Sensitivity is an issue common to all measurement techniques, though the expansive toolkit available to SPR for signal enhancement is bringing many previously undetectable compounds to light. Like the interface itself, however, there are many considerations that must be taken into account when designing an enhancing agent for SPR. These include an assessment of the ease of conjugating enhancing entities with a biorecognition element and determination of the best approach that will result in stable and reproducible platforms for analysis, with minimal nonspecific binding to the sensor surface or matrix. With these parameters optimized, enhanced SPR analysis has great potential in the biosensing field to enable ultrasensitive limits of detection (e.g., subattomolar and single molecule) within rapid time frames. Further integrations of advanced sample handling techniques, including magnetic beads for rapid analyte capture, and microfluidics capable of sample sorting and manipulation, are expected to assist in these efforts. However, SPR as a field is not infallible, and hyphenated analyses with complementary tools, along with method developments for streamlined integrations, are dramatically bolstering its informational power. We expect SPR, or variations of the technique, to reach the hands of exponentially more researchers in the next decade and the growth pattern seen so far (Figure 1) to continue, as its exceptional and growing versatility renders it more desirable for widespread adoption within the measurement and imaging sciences.

Acknowledgments

The authors gratefully acknowledge financial support from the National Science Foundation (CHE-1413449). S.S.H. was supported by a University of California, Riverside (UCR) Dissertation Year Program (DYP) fellowship and an NIEHS T32 training grant (T32 ES018827).

Biographies

Samuel S. Hinman obtained his Ph.D. in Environmental Toxicology under the supervision of Prof. Quan Cheng at the University of California, Riverside in 2017, and his B.S. in Chemistry from the University of Virginia in 2012. His research interests include interface development for surface plasmon resonance and mass spectrometric analyses, with a focus on expanding the utility of supported lipid membrane platforms.

Kristy S. McKeating obtained her Ph.D. at the University of Strathclyde in 2013 under the supervision of Prof. Karen Faulds, after which she moved into her first postdoctoral position at the University of Montreal. There she worked alongside Prof. Jean-François Masson on the development of portable SPR instrumentation for clinical diagnostics, before joining Prof. Quan Cheng at the University of California, Riverside in 2016, where her research has focused on the use of nanoparticle enhanced SPR imaging as a multibiomarker detection platform.

Quan Cheng received his B.S. and M.S. degree in chemistry from Nanjing University, China, and Ph.D. in analytical chemistry from the University of Florida in 1995. After a postdoctoral stint at UC Berkeley, he worked as a staff scientist at Lawrence Berkeley National Laboratory from 1997 to 2001. He joined the chemistry faculty of UC Riverside as an assistant professor in 2001 and was promoted to associate professor in 2007 and

professor in 2010. The research interest of his lab is centered on biosensing technologies with surface plasmon resonance, microarray, electrochemistry, functional materials, and surface-enhanced mass spectrometric methods.

References

1. Li M, Cushing SK, Wu N. Analyst. 2015; 140:386–406. [PubMed: 25365823]
2. Jackman JA, Rahim Ferhan A, Cho NJ. Chem Soc Rev. 2017; 46:3615–3660. [PubMed: 28383083]
3. Farka Z, Jurík T, Kovář D, Trnková L, Skládal P. Chem Rev. 2017; 117:9973–10042. [PubMed: 28753280]
4. Maurer T, Adam P-M, Lévêque G. Nanophotonics. 2015; 4:363.
5. Unser S, Bruzas I, He J, Sagle L. Sensors. 2015; 15:15684–15716. [PubMed: 26147727]
6. Zhou W, Gao X, Liu DB, Chen XY. Chem Rev. 2015; 115:10575–10636. [PubMed: 26114396]
7. Masson JF. ACS Sens. 2017; 2:16–30. [PubMed: 28722437]
8. Fenzl C, Hirsch T, Baeumner AJ. TrAC, Trends Anal Chem. 2016; 79:306–316.
9. Zhang P, Chen YP, Wang W, Shen Y, Guo JS. TrAC, Trends Anal Chem. 2016; 85:153–165.
10. Puiu M, Bala C. Sensors. 2016; 16:870.
11. Wang DS, Fan SK. Sensors. 2016; 16:1175.
12. Liedberg B, Nylander C, Lundstrom I. Biosens Bioelectron. 1995; 10:i–ix. [PubMed: 7576432]
13. Kretschmann E, Raether H. Naturforsch, A: Astrophys, Phys Phys Chem. 1968; 23:2135–2136.
14. Hlubina P, Duliakova M, Kadulova M, Ciprian D. Opt Commun. 2015; 354:240–245.
15. Hlubina P, Ciprian D. Plasmonics. 2017; 12:1071–1078.
16. Bolduc OR, Live LS, Masson JF. Talanta. 2009; 77:1680–1687. [PubMed: 19159783]
17. Zhao SS, Bukar N, Toulouse JL, Pelechacz D, Robitaille R, Pelletier JN, Masson J-F. Biosens Bioelectron. 2015; 64:664–670. [PubMed: 25441416]
18. Aubé A, Charbonneau DM, Pelletier JN, Masson J-F. ACS Sens. 2016; 1:1358–1365.
19. Brule T, Granger G, Bukar N, Deschenes-Rancourt C, Havard T, Schmitzer AR, Martel R, Masson JF. Analyst. 2017; 142:2161–2168. [PubMed: 28548156]
20. Aubé A, Campbell S, Schmitzer AR, Claing A, Masson J-F. Analyst. 2017; 142:2343–2353. [PubMed: 28560368]
21. Ozdemir SK, Turhan-Sayan G. J Lightwave Technol. 2003; 21:805–814.
22. Naimushin AN, Soelberg SD, Bartholomew DU, Elkind JL, Furlong CE. Sens Actuators, B. 2003; 96:253–260.
23. Schlereth DD. J Electroanal Chem. 1999; 464:198–207.
24. Wu C, Rehman FU, Li J, Ye J, Zhang Y, Su M, Jiang H, Wang X. ACS Appl Mater Interfaces. 2015; 7:24848–24854. [PubMed: 26492438]
25. Luo W, Chen S, Chen L, Li HL, Miao PC, Gao HY, Hu ZL, Li M. Opt Express. 2017; 25:12733–12742. [PubMed: 28786627]
26. Peterlinz KA, Georgiadis R. Opt Commun. 1996; 130:260–266.
27. Zacher T, Wischerhoff E. Langmuir. 2002; 18:1748–1759.
28. Nizamov S, Mirsky VM. Biosens Bioelectron. 2011; 28:263–269. [PubMed: 21820884]
29. Liu AP, Peng JL, Li GS. Appl Phys Lett. 2014; 104:211103.
30. Rupert DLM, Shelke GV, Emilsson G, Claudio V, Block S, Lasser C, Dahlin A, Lotvall JO, Bally M, Zhdanov VP, Hook F. Anal Chem. 2016; 88:9980–9988.
31. Wilkop T, Wang ZZ, Cheng Q. Langmuir. 2004; 20:11141–11148. [PubMed: 15568869]
32. Al Mubarak ZH, Ramesh R, Liu L, Krishnan S. J Colloid Interface Sci. 2015; 460:209–213. [PubMed: 26321574]
33. Spoto G, Minunni M. J Phys Chem Lett. 2012; 3:2682–2691. [PubMed: 26295892]
34. Fasoli JB, Corn RM. Langmuir. 2015; 31:9527–9536. [PubMed: 25641598]

35. Peungthum P, Sudprasert K, Amarit R, Somboonkaew A, Sutapun B, Vongsakulyanon A, Seedacoon W, Kitpoka P, Kunakorn M, Srikhirin T. Analyst. 2017; 142:1471–1481. [PubMed: 28345691]
36. Tokarzewicz A, Romanowicz L, Sveklo I, Gorodkiewicz E. Anal Methods. 2016; 8:6428–6435.
37. Zhang F, Wang S, Yin L, Yang Y, Guan Y, Wang W, Xu H, Tao N. Anal Chem. 2015; 87:9960–9965. [PubMed: 26368334]
38. Walgama C, Al Mubarak ZH, Zhang B, Akinwale M, Pathiranage A, Deng JP, Berlin KD, Benbrook DM, Krishnan S. Anal Chem. 2016; 88:3130–3135. [PubMed: 26886845]
39. Liu CJ, Wang X, Xu JY, Chen Y. Anal Chem. 2016; 88:10011–10018.
40. Abadian PN, Yildirim N, Gu AZ, Goluch ED. Biosens Bioelectron. 2015; 74:808–814. [PubMed: 26232675]
41. Melaine F, Saad M, Faucher S, Tabrizian M. Anal Chem. 2017; 89:7802–7807. [PubMed: 28682593]
42. Hu F, Xu J, Chen Y. Anal Chem. 2017; 89:10071–10077. [PubMed: 28825962]
43. Manuel G, Luptak A, Corn RM. J Phys Chem C. 2016; 120:20984–20990.
44. Hinman SS, Ruiz CJ, Drakakaki G, Wilkop TE, Cheng Q. ACS Appl Mater Interfaces. 2015; 7:17122–17130. [PubMed: 26193345]
45. Abadian PN, Kelley CP, Goluch ED. Anal Chem. 2014; 86:2799–2812. [PubMed: 24502446]
46. Abadian PN, Tandogan N, Jamieson JJ, Goluch ED. Biomicrofluidics. 2014; 8:021804. [PubMed: 24753735]
47. Abadian PN, Goluch ED. Anal Methods. 2015; 7:115–122.
48. Zhang PF, Liu L, He YH, Ji YH, Guo J, Ma H. Plasmonics. 2016; 11:771–779.
49. Deng SJ, Wang P, Liu SN, Zhao TZ, Xu SZ, Guo MJ, Yu XL. Sensors. 2016; 16:964.
50. Sereda A, Moreau J, Boulade M, Olivero A, Canva M, Maillart E. Sens Actuators, B. 2015; 209:208–211.
51. Zeng YJ, Wang L, Wu SY, He JN, Qu JL, Li XJ, Ho HP, Gu DY, Gao BZ, Shao YH. Opt Express. 2016; 24:28303–28311. [PubMed: 27958541]
52. Chen KQ, Zeng YJ, Wang L, Gu DY, He JN, Wu SY, Ho HP, Li XJ, Qu JL, Gao BZ, Shao YH. J Biomed Opt. 2016; 21:127003. [PubMed: 27936268]
53. Zeng YJ, Wang L, Wu SY, He JA, Qu JL, Li XJ, Ho HP, Gu DY, Gao BZ, Shao YH. Sensors. 2017; 17:90.
54. Zybin A, Kuritsyn YA, Gurevich EL, Temchura VV, Uberla K, Niemax K. Plasmonics. 2010; 5:31–35.
55. Kano H, Mizuguchi S, Kawata S. J Opt Soc Am B. 1998; 15:1381–1386.
56. Huang B, Yu F, Zare RN. Anal Chem. 2007; 79:2979–2983. [PubMed: 17309232]
57. Syal K, Wang W, Shan XN, Wang SP, Chen HY, Tao NJ. Biosens Bioelectron. 2015; 63:131–137. [PubMed: 25064821]
58. Syal K, Iriya R, Yang YZ, Yu H, Wang SP, Haydel SE, Chen HY, Tao NJ. ACS Nano. 2016; 10:845–852. [PubMed: 26637243]
59. Yuan L, Wang X, Fang YM, Liu CB, Jiang D, Wo X, Wang W, Chen HY. Anal Chem. 2016; 88:2321–2326. [PubMed: 26758648]
60. Wo X, Li ZM, Jiang YY, Li MH, Su YW, Wang W, Tao NJ. Anal Chem. 2016; 88:2380–2385. [PubMed: 26781326]
61. Halpern AR, Wood JB, Wang Y, Corn RM. ACS Nano. 2014; 8:1022–1030. [PubMed: 24350885]
62. Cho K, Fasoli JB, Yoshimatsu K, Shea KJ, Corn RM. Anal Chem. 2015; 87:4973–4979. [PubMed: 25844641]
63. Maley AM, Terada Y, Onogi S, Shea KJ, Miura Y, Corn RM. J Phys Chem C. 2016; 120:16843–16849.
64. Viitala L, Maley AM, Fung HWM, Corn RM, Viitala T, Murtomaki L. J Phys Chem C. 2016; 120:25958–25966.
65. Maley AM, Lu GJ, Shapiro MG, Corn RM. ACS Nano. 2017; 11:7447–7456. [PubMed: 28692253]

66. Yu H, Shan XN, Wang SP, Tao NJ. Anal Chem. 2017; 89:2704–2707. [PubMed: 28194944]
67. Shan XN, Fang YM, Wang SP, Guan Y, Chen HY, Tao NJ. Nano Lett. 2014; 14:4151–4157. [PubMed: 24942903]
68. Fang YM, Chen S, Wang W, Shan XN, Tao NJ. Angew Chem, Int Ed. 2015; 54:2538–2542.
69. Jorgenson RC, Yee SS. Sens Actuators, B. 1993; 12:213–220.
70. Zhao J, Cao SQ, Liao CR, Wang Y, Wang GJ, Xu XZ, Fu CL, Xu GW, Lian JR, Wang YP. Sens Actuators, B. 2016; 230:206–211.
71. Haddouche I, Cherbi L, Ferhat ML. Opt Commun. 2017; 402:618–623.
72. Velazquez-Gonzalez JS, Monzon-Hernandez D, Moreno-Hernandez D, Martinez-Pinon F, Hernandez-Romano I. Sens Actuators, B. 2017; 242:912–920.
73. Chen SM, Liu Y, Liu ZG, Chu SW, Peng W. Appl Opt. 2016; 55:8571–8575. [PubMed: 27828137]
74. Liu Y, Chen SM, Liu Q, Masson JF, Peng W. Opt Express. 2015; 23:20540–20548. [PubMed: 26367906]
75. Hinman SS, McKeating KS, Cheng Q. Anal Chem. 2017; 89:4272–4279. [PubMed: 28316233]
76. Hinman SS, Ruiz CJ, Cao Y, Ma MC, Tang JJ, Laurini E, Posocco P, Giorgio S, Pricl S, Peng L, Cheng Q. ACS Appl Mater Interfaces. 2017; 9:1029–1035. [PubMed: 27957833]
77. Adducci BA, Gruszewski HA, Khatibi PA, Schmale DG. Biosens Bioelectron. 2016; 78:160–166. [PubMed: 26606307]
78. Devanarayanan VP, Manjuladevi V, Gupta RK. Sens Actuators, B. 2016; 227:643–648.
79. Michel D, Xiao F, Alameh K. Sens Actuators, B. 2017; 246:258–261.
80. Joshi S, Annida RM, Zuilhof H, van Beek TA, Nielen MWF. J Agric Food Chem. 2016; 64:8263–8271. [PubMed: 27709929]
81. Colas F, Crassous MP, Laurent S, Litaker RW, Rinnert E, Le Gall E, Lunven M, Delauney L, Compere C. Limnol Oceanogr: Methods. 2016; 14:456–465.
82. Preechaburana P, Gonzalez MC, Suska A, Filippini D. Angew Chem, Int Ed. 2012; 51:11585–11588.
83. Liu Y, Liu Q, Chen SM, Cheng F, Wang HQ, Peng W. Sci Rep. 2015; 5:12864. [PubMed: 26255778]
84. Bremer K, Roth B. Opt Express. 2015; 23:17179–17184. [PubMed: 26191726]
85. Zhang J, Khan I, Zhang Q, Liu X, Dostalek J, Liedberg B, Wang Y. Biosens Bioelectron. 2018; 99:312–317. [PubMed: 28787676]
86. Guner H, Ozgur E, Kokturk G, Celik M, Esen E, Topal AE, Ayas S, Uludag Y, Elbuken C, Dana A. Sens Actuators, B. 2017; 239:571–577.
87. Lu MD, Liang YZ, Qian SY, Li LX, Jing ZG, Masson JF, Peng W. Plasmonics. 2017; 12:663–673.
88. Steinicke F, Oltmann-Norden I, Watzig H. Anal Biochem. 2017; 530:94–103. [PubMed: 28501475]
89. McPeak KM, Jayanti SV, Kress SJP, Meyer S, Iotti S, Rossinelli A, Norris DJ. ACS Photonics. 2015; 2:326–333. [PubMed: 25950012]
90. Blaber MG, Arnold MD, Ford MJ. J Phys : Condens Matter. 2010; 22:095501. [PubMed: 21389416]
91. Naik GV, Shalaev VM, Boltasseva A. Adv Mater. 2013; 25:3264–3294. [PubMed: 23674224]
92. Biednov M, , Lebyedyeva T, , Pavlo S. In Proc SPIE 9506, ptical Sensors 2015 SPIE; Bellingham, WA: 2015 95061P
93. Tanabe I, Tanaka YY, Ryoki T, Watari K, Goto T, Kikawada M, Inami W, Kawata Y, Ozaki Y. Opt Express. 2016; 24:21886–21896. [PubMed: 27661924]
94. Tanabe I, Tanaka YY, Watari K, Hanulia T, Goto T, Inami W, Kawata Y, Ozaki Y. Sci Rep. 2017; 7:5934. [PubMed: 28725007]
95. Geiss FA, , Fossati S, , Khan I, , Gisbert Quilis N, , Knoll W, , Dostalek J. In Proc SPIE 10231, Optical Sensors 2017 SPIE; Bellingham, WA: 2017 1023107
96. Gong C, Leite MS. ACS Photonics. 2016; 3:507–513.
97. Gao CB, Hu YX, Wang MS, Chi MF, Yin YD. J Am Chem Soc. 2014; 136:7474–7479. [PubMed: 24821567]
98. Bai Y, Gao CB, Yin L. Nanoscale. 2017; 9:14875. [PubMed: 28975172]

99. Gu D, Zhang C, Wu YK, Guo LJ. ACS Nano. 2014; 8:10343–10351. [PubMed: 25211394]
100. Appusamy K, Swartz M, Blair S, Nahata A, Shumaker-Parry JS, Guruswamy S. Opt Mater Express. 2016; 6:3180–3192.
101. Gupta G, Kondoh J. Sens Actuators, B. 2007; 122:381–388.
102. Pandey AK, Sharma AK, Basu R. J Phys D: Appl Phys. 2017; 50:185103.
103. Gupta G, Sugimoto M, Matsui Y, Kondoh J. Sens Actuators, B. 2008; 130:689–695.
104. Obreja P, Cristea D, Kusko M, Dinescu A. J Opt A: Pure Appl Opt. 2008; 10:064010.
105. Lan GQ, Liu SG, Zhang XR, Wang YX, Song YL. Rev Sci Instrum. 2015; 86:025006. [PubMed: 25725880]
106. Lan GQ, Liu SG, Ma Y, Zhang XR, Wang YX, Song YL. Opt Commun. 2015; 352:49–54.
107. Gross B, Lockwood SY, Spence DM. Anal Chem. 2017; 89:57–70. [PubMed: 28105825]
108. Kotz F, Arnold K, Bauer W, Schild D, Keller N, Sachsenheimer K, Nargang TM, Richter C, Helmer D, Rapp BE. Nature. 2017; 544:337–339. [PubMed: 28425999]
109. Hinman SS, McKeating KS, Cheng Q. Plasmonic Sensing with 3D Printed Optics. 2017 unpublished work.
110. Abali F, Stevens M, Tibbe AGJ, Terstappen LWMM, van der Velde PN, Schasfoort RBM. Anal Biochem. 2017; 531:45–47. [PubMed: 28545866]
111. Abbas A, Linman MJ, Cheng Q. Anal Chem. 2011; 83:3147–3152. [PubMed: 21417424]
112. Linman MJ, Abbas A, Roberts CC, Cheng Q. Anal Chem. 2011; 83:5936–5943. [PubMed: 21711025]
113. Shen L, Wang YN, Lin CI, Liu HW, Guo A, Zhu XY. ACS Chem Biol. 2014; 9:1877–1884. [PubMed: 24949798]
114. Perez L, Mettry M, Hinman SS, Byers SR, McKeating KS, Caulkins BG, Cheng Q, Hooley RJ. Soft Matter. 2017; 13:3966–3974. [PubMed: 28512660]
115. Kim S, Lee HJ. Anal Chem. 2017; 89:6624–6630. [PubMed: 28520392]
116. Ulman A. Chem Rev. 1996; 96:1533–1554. [PubMed: 11848802]
117. Yang C-T, Pourhassan-Moghaddam M, Wu L, Bai P, Thierry B. ACS Sens. 2017; 2:635–640. [PubMed: 28723162]
118. Iijima M, Kuroda SI. Biosens Bioelectron. 2017; 89:810–821. [PubMed: 27818052]
119. Forest S, Breault-Turcot J, Chaurand P, Masson JF. Anal Chem. 2016; 88:2072–2079. [PubMed: 26765517]
120. Kim S, Wark AW, Lee HJ. Anal Chem. 2016; 88:7793–7799. [PubMed: 27399254]
121. Liu B, Liu X, Shi S, Huang R, Su R, Qi W, He Z. Acta Biomater. 2016; 40:100–118. [PubMed: 26921775]
122. Safazadeh L, Zehuri VEF, Pautler SP, Hastings JT, Berron BJ. Langmuir. 2016; 32:8034–8041. [PubMed: 27463892]
123. Farka Z, Jurík T, Pastucha M, Skladal P. Anal Chem. 2016; 88:11830–11836. [PubMed: 27813408]
124. Li S, Yang M, Zhou W, Johnston TG, Wang R, Zhu J. Appl Surf Sci. 2015; 355:570–576.
125. Abbas A, Linman MJ, Cheng Q. Biosens Bioelectron. 2011; 26:1815–1824. [PubMed: 20951566]
126. Wang Y, Partridge A, Wu Y. Anal Biochem. 2016; 508:46–49. [PubMed: 27288558]
127. Stebunov YV, Aftenieva OA, Arsenin AV, Volkov VS. ACS Appl Mater Interfaces. 2015; 7:21727–21734. [PubMed: 26358000]
128. Chiu N-F, Fan S-Y, Yang C-D, Huang T-Y. Biosens Bioelectron. 2017; 89:370–376. [PubMed: 27396822]
129. Lee H, Dellatore SM, Miller WM, Messersmith PB. Science. 2007; 318:426–430. [PubMed: 17947576]
130. Wood JB, Szyndler MW, Halpern AR, Cho K, Corn RM. Langmuir. 2013; 29:10868–10873. [PubMed: 23902428]
131. Shi S, Wang L, Su R, Liu B, Huang R, Qi W, He Z. Biosens Bioelectron. 2015; 74:454–460. [PubMed: 26164491]

132. Toma M, Tawa K. ACS Appl Mater Interfaces. 2016; 8:22032–22038. [PubMed: 27484114]
133. Ye H, Xia Y, Liu Z, Huang R, Su R, Qi W, Wang L, He Z. J Mater Chem B. 2016; 4:4084–4091.
134. He L, Pagneux Q, Larroulet I, Serrano AY, Pesquera A, Zurutuza A, Mandler D, Boukherroub R, Szunerits S. Biosens Bioelectron. 2017; 89:606–611. [PubMed: 26852830]
135. Huang R, Liu X, Ye H, Su R, Qi W, Wang L, He Z. Langmuir. 2015; 31:12061–12070. [PubMed: 26488547]
136. Dang Y, Xing CM, Quan M, Wang YB, Zhang SP, Shi SQ, Gong YK. J Mater Chem B. 2015; 3:4181–4190.
137. Lowe S, O'Brien-Simpson NM, Connal LA. Polym Chem. 2015; 6:198–212.
138. Pop-Georgievski O, Verreault D, Diesner M-O, Proks V, Heissler S, Rypáček F, Koelsch P. Langmuir. 2012; 28:14273–14283. [PubMed: 22989020]
139. Vaisocherova H, Brynda E, Homola J. Anal Bioanal Chem. 2015; 407:3927–3953. [PubMed: 25821150]
140. Parrillo V, de los Santos Pereira A, Riedel T, Rodriguez-Emmenegger C. Anal Chim Acta. 2017; 971:78–87. [PubMed: 28456286]
141. Shao Q, Jiang S. Adv Mater. 2015; 27:15–26. [PubMed: 25367090]
142. Yang W, Xue H, Li W, Zhang J, Jiang S. Langmuir. 2009; 25:11911–11916. [PubMed: 19583183]
143. Vaisocherová H, Šípová H, Víšová I, Bocková M, Špringer T, Laura Ermini M, Song X, Krejčík Z, Chrastinová L, Pastva O, Pimková K, Dostálová Merkerová M, Dyr JE, Homola J. Biosens Bioelectron. 2015; 70:226–231. [PubMed: 25829219]
144. Vaisocherová H, Ševců V, Adam P, Špačková B, Hegnerová K, de los Santos Pereira A, Rodriguez-Emmenegger C, Riedel T, Houska M, Brynda E, Homola J. Biosens Bioelectron. 2014; 51:150–157. [PubMed: 23954672]
145. Aube A, Breault-Turcot J, Chaurand P, Pelletier JN, Masson JF. Langmuir. 2013; 29:10141–10148. [PubMed: 23845017]
146. Ye H, Wang L, Huang R, Su R, Liu B, Qi W, He Z. ACS Appl Mater Interfaces. 2015; 7:22448–22457. [PubMed: 26407144]
147. Bolduc OR, Pelletier JN, Masson JF. Anal Chem. 2010; 82:3699–3706. [PubMed: 20353164]
148. Wiarachai O, Vilaivan T, Iwasaki Y, Hoven VP. Langmuir. 2016; 32:1184–1194. [PubMed: 26695478]
149. Dang Y, Quan M, Xing C-M, Wang Y-B, Gong Y-K. J Mater Chem B. 2015; 3:2350–2361.
150. Akkahat P, Kiatkamjornwong S, Yusa S-I, Hoven VP, Iwasaki Y. Langmuir. 2012; 28:5872–5881. [PubMed: 22364521]
151. Lísalová H, Brynda E, Houska M, Víšová I, Mrkvová K, Song XC, Gedeonova E, Surman F, Riedel T, Pop-Georgievski O, Homola J. Anal Chem. 2017; 89:3524–3531. [PubMed: 28233990]
152. Vaisocherová-Lísalová H, Surman F, Víšová I, Vala M, Springer T, Ermini ML, Šípová H, Šedivák P, Houska M, Riedel T, Pop-Georgievski O, Brynda E, Homola J. Anal Chem. 2016; 88:10533–10539. [PubMed: 27689386]
153. Rodriguez-Emmenegger C, Avramenko OA, Brynda E, Skvor J, Alles AB. Biosens Bioelectron. 2011; 26:4545–4551. [PubMed: 21664120]
154. Vaisocherová-Lísalová H, Víšová I, Ermini ML, Špringer T, Song XC, Mrázek J, Lamačová J, Scott Lynn N, Šedivák P, Homola J. Biosens Bioelectron. 2016; 80:84–90. [PubMed: 26807521]
155. Hinman SS, Cheng Q. J Electroanal Chem. 2016; 781:136–146.
156. Castellana ET, Cremer PS. Surf Sci Rep. 2006; 61:429–444.
157. Liu Y, Cheng Q. Anal Chem. 2012; 84:3179–3186. [PubMed: 22439623]
158. Rebaud S, Maniti O, Girard-Egrot AP. Biochimie. 2014; 107:135–142. [PubMed: 24998327]
159. Phillips KS, Han JH, Martinez M, Wang ZZ, Carter D, Cheng Q. Anal Chem. 2006; 78:596–603. [PubMed: 16408945]
160. Linman MJ, Culver SP, Cheng Q. Langmuir. 2009; 25:3075–3082. [PubMed: 19437774]
161. Han JH, Taylor JD, Phillips KS, Wang X, Feng P, Cheng Q. Langmuir. 2008; 24:8127–8133. [PubMed: 18605744]

162. Phillips KS, Wilkop T, Wu JJ, Al-Kaysi RO, Cheng Q. J Am Chem Soc. 2006; 128:9590–9591. [PubMed: 16866487]
163. Perez L, Ghang YJ, Williams PB, Wang Y, Cheng Q, Hooley RJ. Langmuir. 2015; 31:11152–11157. [PubMed: 26436343]
164. Ghang Y-J, Perez L, Morgan MA, Si F, Hamdy OM, Beecher CN, Larive CK, Julian RR, Zhong W, Cheng Q, Hooley RJ. Soft Matter. 2014; 10:9651–9656. [PubMed: 25366572]
165. Ghang Y-J, Lloyd JJ, Moehlig MP, Arguelles JK, Mettry M, Zhang X, Julian RR, Cheng Q, Hooley RJ. Langmuir. 2014; 30:10161–10166. [PubMed: 25130415]
166. McKeating KS, Aube A, Masson J-F. Analyst. 2016; 141:429–449. [PubMed: 26631282]
167. Zeng S, Baillargeat D, Ho H-P, Yong K-T. Chem Soc Rev. 2014; 43:3426–3452. [PubMed: 24549396]
168. Wu B, Jiang R, Wang Q, Huang J, Yang X, Wang K, Li W, Chen N, Li Q. Chem Commun. 2016; 52:3568–3571.
169. Li R, Feng F, Chen Z-Z, Bai Y-F, Guo F-F, Wu F-Y, Zhou G. Talanta. 2015; 140:143–149. [PubMed: 26048836]
170. Karczmarczyk A, Dubiak-Szepietowska M, Vorobii M, Rodriguez-Emmenegger C, Dostálek J, Feller K-H. Biosens Bioelectron. 2016; 81:159–165. [PubMed: 26945182]
171. Zeng SW, Yong KT, Roy I, Dinh XQ, Yu X, Luan F. Plasmonics. 2011; 6:491–506.
172. Gupta A, Moyano DF, Parnsubsakul A, Papadopoulos A, Wang LS, Landis RF, Das R, Rotello VM. ACS Appl Mater Interfaces. 2016; 8:14096–14101. [PubMed: 27191946]
173. Kwon MJ, Lee J, Wark AW, Lee HJ. Anal Chem. 2012; 84:1702–1707. [PubMed: 22224823]
174. Jang HR, Wark AW, Baek SH, Chung BH, Lee HJ. Anal Chem. 2014; 86:814–819. [PubMed: 24328254]
175. Baek SH, Wark AW, Lee HJ. Anal Chem. 2014; 86:9824–9829. [PubMed: 25186782]
176. Reiner AT, Ferrer N-G, Venugopalan P, Lai RC, Lim SK, Dostalek J. Analyst. 2017; 142:3913. [PubMed: 28920599]
177. Liu X, Hu Y, Zheng S, Liu Y, He Z, Luo F. Sens Actuators, B. 2016; 230:191–198.
178. Zou F, Wang X, Qi F, Koh K, Lee J, Zhou H, Chen H. Sens Actuators, B. 2017; 250:356–363.
179. Chen H, Qi F, Zhou H, Jia S, Gao Y, Koh K, Yin Y. Sens Actuators, B. 2015; 212:505–511.
180. Fenzl C, Hirsch T, Baeumner AJ. Anal Chem. 2015; 87:11157–11163. [PubMed: 26455696]
181. Fenzl C, Genslein C, Domonkos C, Edwards KA, Hirsch T, Baeumner AJ. Analyst. 2016; 141:5265–5273. [PubMed: 27359168]
182. Linman MJ, Sugerman K, Cheng Q. Sens Actuators, B. 2010; 145:613–619.
183. Ding X, Cheng W, Li Y, Wu J, Li X, Cheng Q, Ding S. Biosens Bioelectron. 2017; 87:345–351. [PubMed: 27587359]
184. Sun W, Song W, Guo X, Wang Z. Anal Chim Acta. 2017; 978:42–47. [PubMed: 28595725]
185. Zeng K, Li H, Peng Y. Microchim Acta. 2017; 184:2637–2644.
186. Wang Q, Liu R, Yang X, Wang K, Zhu J, He L, Li Q. Sens Actuators, B. 2016; 223:613–620.
187. Chang C-C, Chen C-Y, Chuang T-L, Wu T-H, Wei S-C, Liao H, Lin C-W. Biosens Bioelectron. 2016; 78:200–205. [PubMed: 26609945]
188. He P, Qiao W, Liu L, Zhang S. Chem Commun. 2014; 50:10718–10721.
189. Couture M, Live LS, Dhawan A, Masson JF. Analyst. 2012; 137:4162–4170. [PubMed: 22832550]
190. Masson J-F, Murray-Methot M-P, Live LS. Analyst. 2010; 135:1483–1489. [PubMed: 20358096]
191. Correia-Ledo D, Gibson KF, Dhawan A, Couture M, Vo-Dinh T, Graham D, Masson J-F. J Phys Chem C. 2012; 116:6884–6892.
192. Couture M, Liang Y, Poirier Richard H-P, Faid R, Peng W, Masson J-F. Nanoscale. 2013; 5:12399–12408. [PubMed: 24162773]
193. Breault-Turcot J, Masson J-F. Anal Bioanal Chem. 2012; 403:1477–1484. [PubMed: 22526642]
194. Couture M, Ray KK, Poirier-Richard H-P, Crofton A, Masson J-F. ACS Sens. 2016; 1:287–294.
195. Wu Q, Li S, Sun Y, Wang J. Microchim Acta. 2017; 184:2395–2402.

196. Singh M, Holzinger M, Tabrizian M, Winters S, Berner NC, Cosnier S, Duesberg GS. J Am Chem Soc. 2015; 137:2800–2803. [PubMed: 25679322]
197. Wu L, Guo J, Wang Q, Lu S, Dai X, Xiang Y, Fan D. Sens Actuators, B. 2017; 249:542–548.
198. Yuan P-X, Deng S-Y, Yao C-G, Wan Y, Cosnier S, Shan D. Biosens Bioelectron. 2017; 89:319–325. [PubMed: 27471143]
199. Wu Q, Song D, Zhang D, Sun Y. Microchim Acta. 2016; 183:2177–2184.
200. Hu W, He G, Zhang H, Wu X, Li J, Zhao Z, Qiao Y, Lu Z, Liu Y, Li CM. Anal Chem. 2014; 86:4488–4493. [PubMed: 24712824]
201. Stigter ECA, de Jong GJ, van Bennekom WP. TrAC, Trends Anal Chem. 2013; 45:107–120.
202. Cao Y, Li YH, Lv DY, Chen XF, Chen LD, Zhu ZY, Chai YF, Zhang JP. Anal Bioanal Chem. 2016; 408:5359–5367. [PubMed: 27225174]
203. Woods LA, Dolezal O, Ren B, Ryan JH, Peat TS, Poulsen SA. J Med Chem. 2016; 59:2192–2204. [PubMed: 26882437]
204. Zhang YD, Li XJ, Nie HG, Yang L, Li Z, Bai Y, Niu L, Song DQ, Liu HW. Anal Chem. 2015; 87:6505–6509. [PubMed: 26067340]
205. Zhang YD, Xu ST, Wen LH, Bai Y, Niu L, Song DQ, Liu HW. Analyst. 2016; 141:3343–3348. [PubMed: 27116712]
206. Breault-Turcot J, Chaurand P, Masson JF. Anal Chem. 2014; 86:9612–9619. [PubMed: 25287274]
207. Anders U, Schaefer JV, Hibti FE, Frydman C, Suckau D, Pluckthun A, Zenobi R. Anal Bioanal Chem. 2017; 409:1827–1836. [PubMed: 27987025]
208. Yang H, Cheng Q. Analyst. 2017; 142:2654–2662. [PubMed: 28692093]
209. Chen C-Y, Hinman SS, Duan J, Cheng Q. Anal Chem. 2014; 86:11942–11945. [PubMed: 25417963]
210. Hinman SS, Chen CY, Duan J, Cheng Q. Nanoscale. 2016; 8:1665–1675. [PubMed: 26694584]
211. Joshi S, Zuilhof H, van Beek TA, Nielen MWF. Anal Chem. 2017; 89:1427–1432. [PubMed: 28208290]
212. Breault-Turcot J, Poirier-Richard HP, Couture M, Pelechacz D, Masson JF. Lab Chip. 2015; 15:4433–4440. [PubMed: 26467689]
213. Liu S, Zhang HY, Liu WM, Zhou BJ, Ma Q, Ge JC, Wu JS, Wang PF. RSC Adv. 2016; 6:65930–65935.
214. Li JF, Li CY, Aroca RF. Chem Soc Rev. 2017; 46:3962–3979. [PubMed: 28639669]
215. Sergelen K, Fossati S, Turupcu A, Oostenbrink C, Liedberg B, Knoll W, Dostalek J. ACS Sens. 2017; 2:916–923. [PubMed: 28750521]
216. Sergelen K, Liedberg B, Knoll W, Dostalek J. Analyst. 2017; 142:2995–3001. [PubMed: 28744534]
217. Wood AJ, Chen B, Pathan S, Bok S, Mathai CJ, Gangopadhyay K, Grant SA, Gangopadhyay S. RSC Adv. 2015; 5:78534–78544.
218. Yuan Y, Guo T, Qiu XH, Tang JH, Huang YY, Zhuang L, Zhou SG, Li ZH, Guan BO, Zhang XM, Albert J. Anal Chem. 2016; 88:7609–7616. [PubMed: 27214753]
219. Laurinavichyute VK, Nizamov S, Mirsky VM. ChemPhysChem. 2017; 18:1552–1560. [PubMed: 28294502]
220. Patskovsky S, Dallaire AM, Meunier M. Sens Actuators, B. 2016; 222:71–77.
221. Hou YT, An JH, Deng CY, Chen S, Xiang J. Anal Bioanal Chem. 2016; 408:4935–4941. [PubMed: 27215638]
222. Liu XW, Yang Y, Wang W, Wang S, Gao M, Wu J, Tao N. Angew Chem, Int Ed. 2017; 56:8855–8859.
223. Fang YM, Wang H, Yu H, Liu XW, Wang W, Chen HY, Tao NJ. Acc Chem Res. 2016; 49:2614–2624. [PubMed: 27662069]
224. Wang Y, Wang H, Chen YH, Wang YX, Chen HY, Shan XN, Tao NJ. J Am Chem Soc. 2017; 139:7244–7249. [PubMed: 28478669]

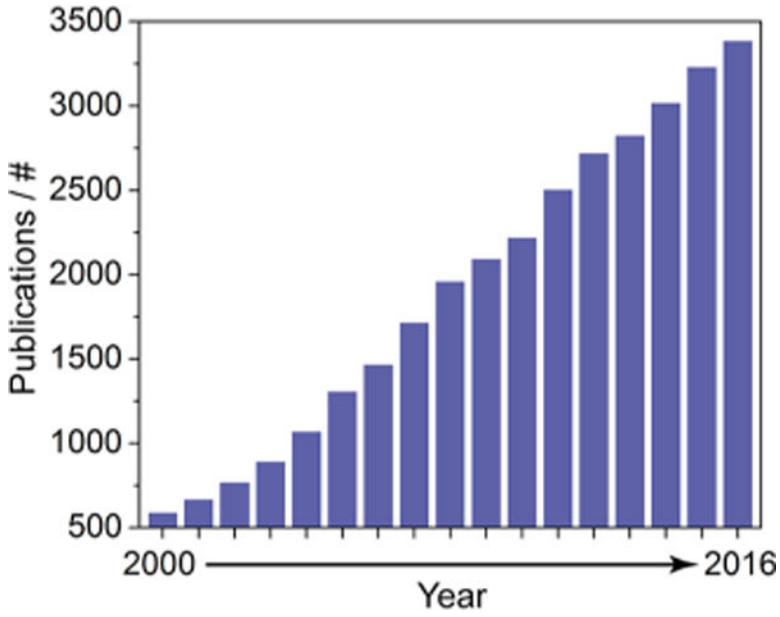

Figure 1.

Growth in surface plasmon resonance publications since 2000. Results were obtained from a topic search on the Web of Science (Clarivate Analytics) using the keywords “surface plasmon resonance” and in a separate field NOT “localized” to exclude publications on localized surface plasmon resonance (LSPR) and surface enhanced Raman spectroscopy (SERS), which operate under related mechanisms.

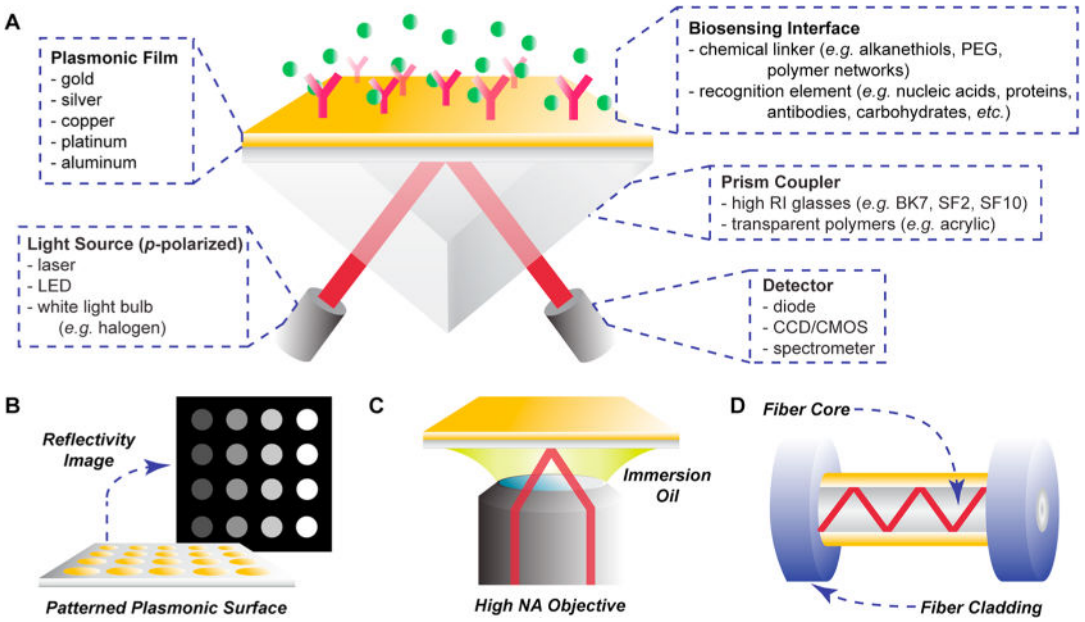

Figure 2.

Common instrumental configurations for surface plasmon resonance. (A) Spectroscopic SPR setup in the Kretschmann configuration, with various component options provided. (B) In SPR imaging, interactions with a patterned plasmonic array are visualized and monitored for changes in reflected light intensity, indicative of molecular binding. (C) SPR microscopy utilizes a high numerical aperture objective to guide incident light toward the gold film at a high angle of incidence. (D) Single mode fiber SPR setup, in which an area of optical fiber cladding is removed and a gold film is deposited.

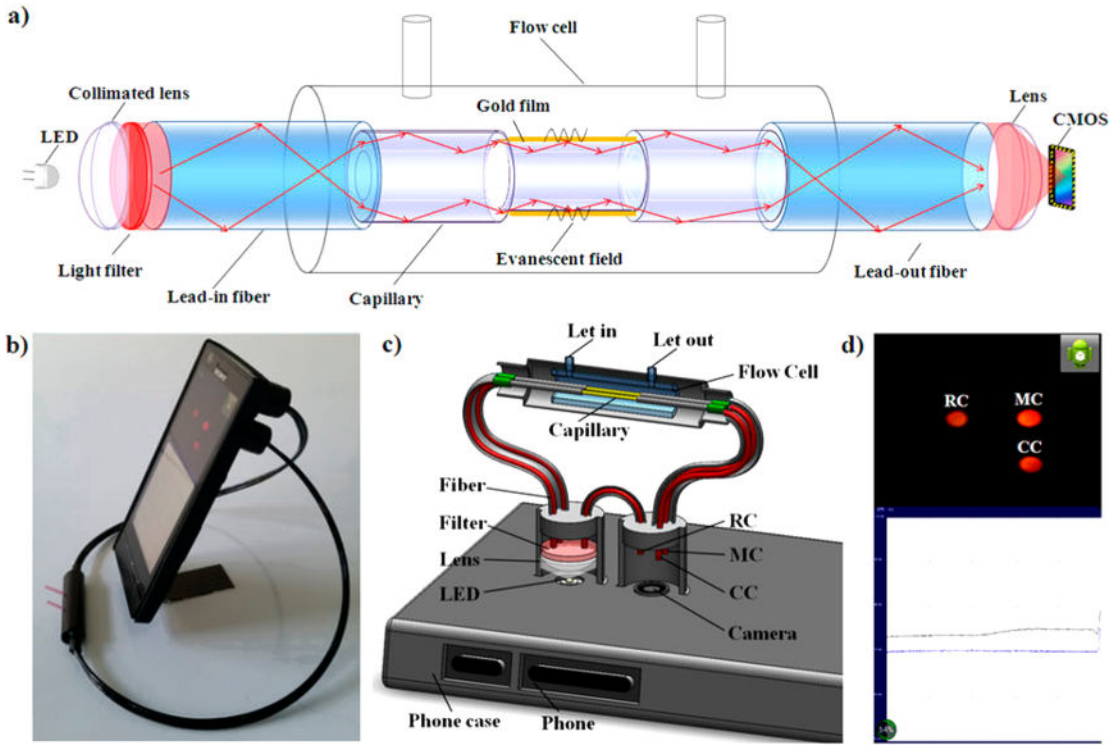

Figure 3.

(a) Schematic of the smart phone-based SPR sensor. (b) Photograph of the SPR sensor installed on an Android-based smart phone. (c) 3D schematic illustration of the internal structure of the opto-mechanical attachment. (d) The camera of the smart phone captures the images of the measurement channel, control channel, and reference channel; then, the images are rapidly processed to obtain the relative intensity. The data points are plotted and displayed on the screen. Reprinted by permission from Macmillan Publishers Ltd.: Scientific Reports, Liu, Y.; Liu, Q.; Chen, S.; Cheng, F.; Wang, H.; Peng, W. *Sci Rep.* 2015, *5*, 12864 (ref [83]).

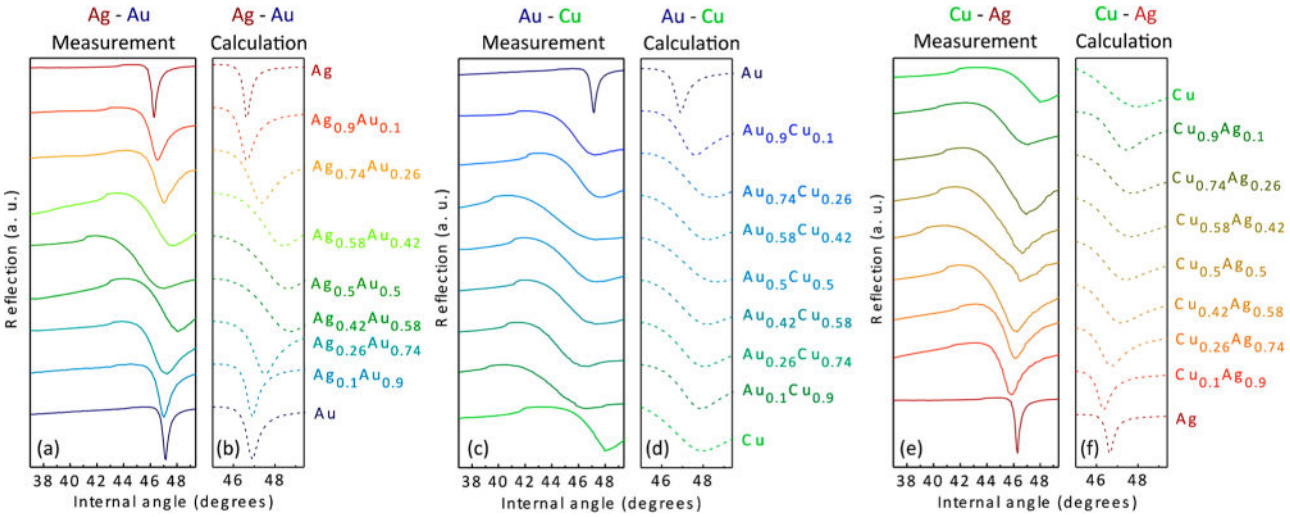

Figure 4.

Surface plasmon polariton excitation in noble metal alloys. Measurements and calculations showing surface plasmon polariton excitation as a function of internal angle in a Kretschmann configuration for (a, b) Ag–Au, (c, d) Au–Cu, and (e, f) Cu–Ag thin films. Light source: 637 nm diode laser *p*-polarized with 3.6 mW. Reprinted from Gong, C.; Leite, M. S. *ACS Photonics* 2016, *3*, 507–513 (ref [96]). Copyright 2016 American Chemical Society.

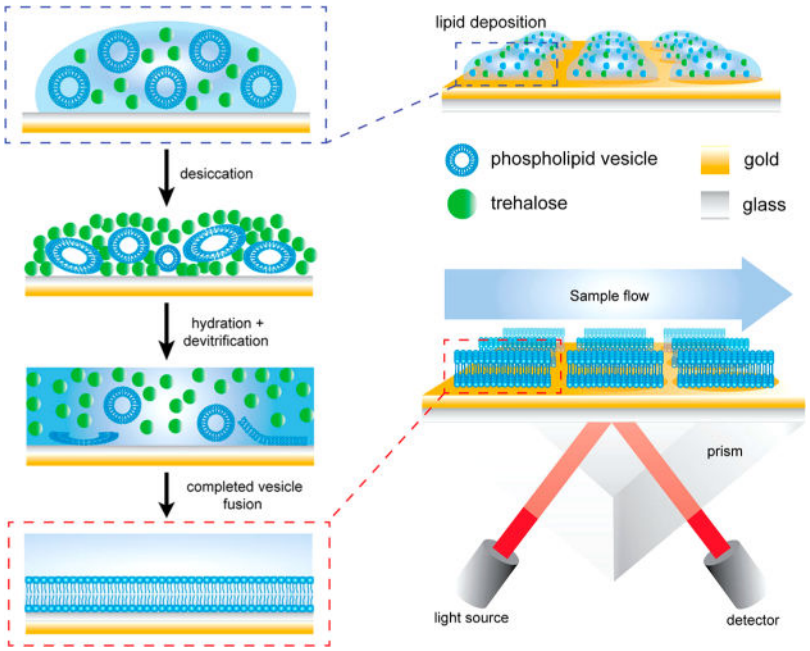

Figure 5.

Schematic diagram showing the process of vesicle deposition, desiccation, and devitrification upon hydration of the trehalose matrix on the modified SPR sensor chips. Each SPR chip is modified with ca. 10 nm of silica, applied by plasma-enhanced chemical vapor deposition, to increase hydrophilicity and provide a fusogenic surface for the SUVs. The devitrification process releasing SUVs takes place in the SPR flow cell environment. Reprinted from Hinman, S. S.; Ruiz, C. J.; Drakakaki, G.; Wilkop, T. E.; Cheng Q. *ACS Appl. Mater. Interfaces* 2015, *7*, 17122–17130 (ref [44]). Copyright 2015 American Chemical Society.

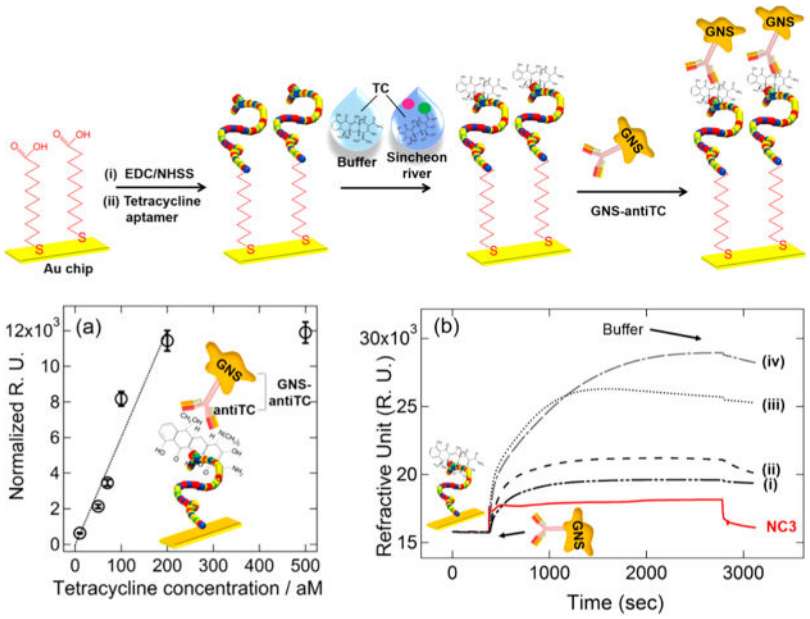

Figure 6.

(Top) Schematic overview of strategy for tetracycline (TC) detection. The TC aptamer was first immobilized on a SPR chip, followed by the covalent attachment of aptamer probes. TC binding was performed in both buffer and Sincheon river samples, followed by the subsequent binding of GNS antiTCs for further SPR signal amplification. (Bottom) (a) Monitoring changes in SPR response (normalized with respect to the average signal of NC signals) where the GNS concentration after the antiTC modification was fixed at 2.41 nM (optical density (OD) = 1.4) for a series of measurements where the SPR chip had already been exposed to different TC target concentrations from 10 aM to 500 aM in buffer. Each data point is the average of at least four repeat measurements. (b) Representative real-time SPR responses for different concentrations of TC. The concentrations of TC were (i) NC, (ii) 50, (iii) 70, (iv) 100 aM. Adapted from Kim, S.; Lee, H. J. *Anal. Chem.* 2017, *89*, 6624–6630 (ref [115]). Copyright 2017 American Chemical Society.

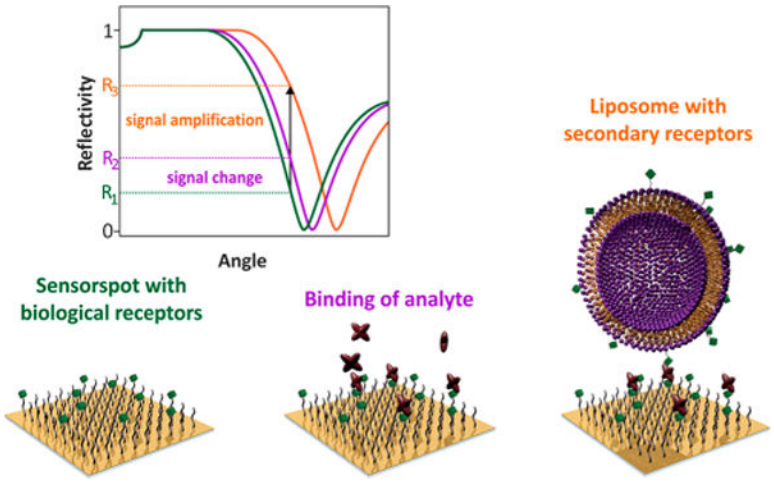

Figure 7.

Sensing scheme for the SPR signal amplification with liposomes. Liposomes are used as label subsequent to the analyte binding to the SPR surface. Although this renders the traditionally label-free SPR method to a label-based detection system, this approach will enable the detection of bound analytes present at low concentration and those providing only minimal changes in RI. Reprinted from Fenzl, C.; Hirsch, T.; Baeumner, A. J. *Anal. Chem.* 2015, *87*, 11157–11163 (ref [180]). Copyright American Chemical Society 2015.

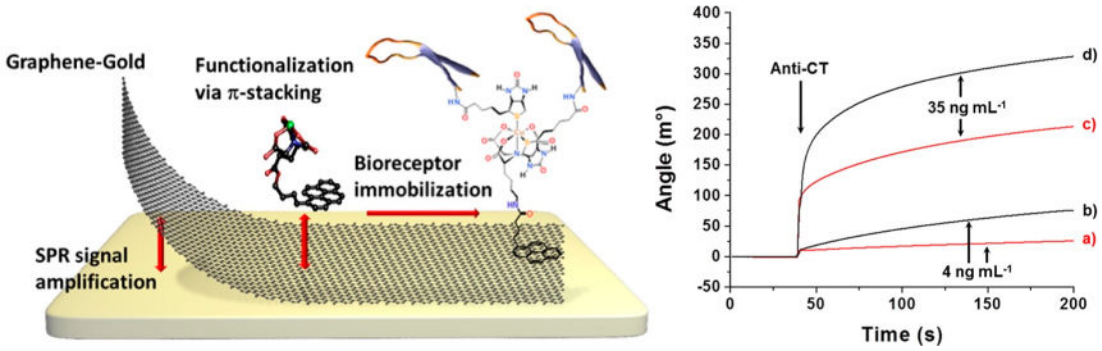

Figure 8.

(Left) Schematic representing the phenomenon of coating gold with monolayer graphene for both signal enhancement and recognition element attachment. (Right) SPR angle shift after anticholera toxin (CT) injection using pure gold (red) and graphene-gold (black) surfaces functionalized with polypyrrole-NTA/Cu^{2+}/b-CT at two different anti-CT concentrations (a, b: 4 ng·mL^{-1}; c, d: 35 ng·mL^{-1}). The polymer film was formed under controlled potential electrolysis (0.95 V, 1 mC·cm^{-2}). Adapted from Singh, M.; Holzinger, M.; Tabrizian, M.; Winters, S.; Berner, N. C.; Cosnier, S.; Duesberg, G. S. *J. Am. Chem. Soc.* 2015, *137*, 2800–2803 (ref [196]). Copyright 2015 American Chemical Society.

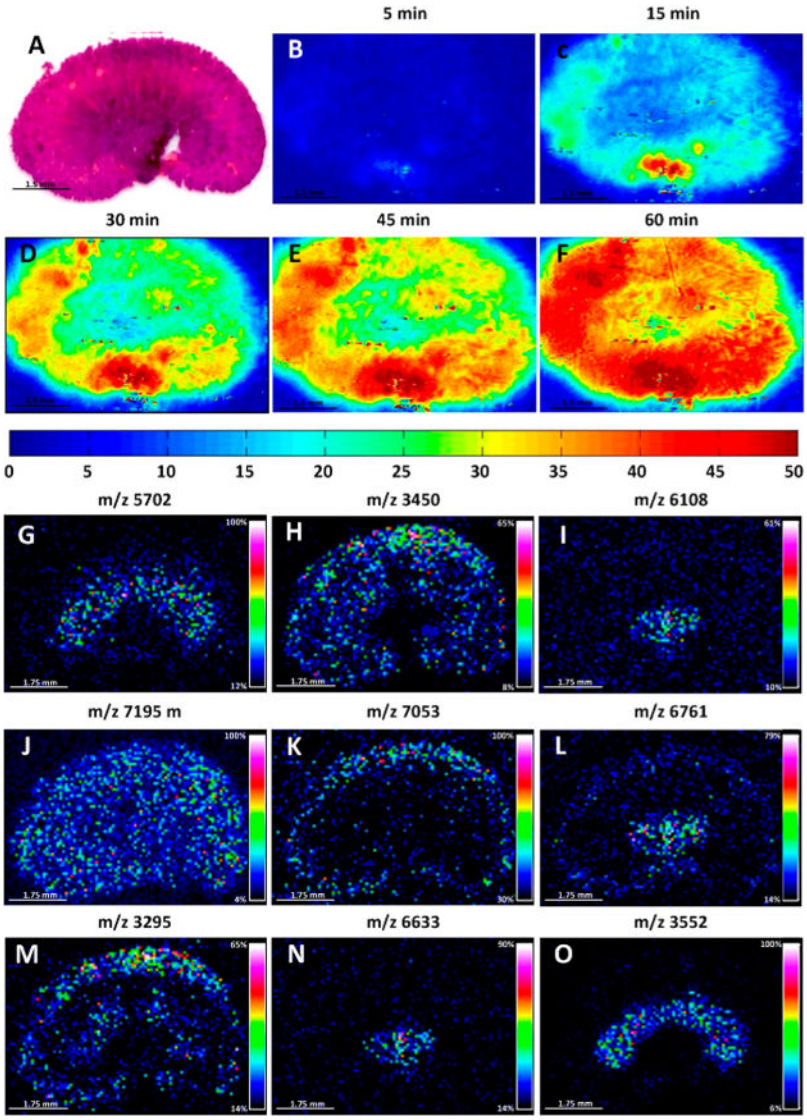

Figure 9.

SPRi-MALDI IMS protein images acquired for a 20 μm thick mouse kidney section. (A) H&E stained kidney section after 60 min of protein transfer. (B–F) SPRi images of the protein imprint at different time intervals (color scale is in ng/cm^2). (G–O) Selected protein MALDI IMS images (100 μm spatial resolution) of the imprint on the SPRi sensor after 60 min of transfer time. Reprinted from Forest, S.; Breault-Turcot, J.; Chaurand, P.; Masson, J.-F. *Anal. Chem.* 2016, *88*, 2072–2079 (ref [119]). Copyright 2016 American Chemical Society.

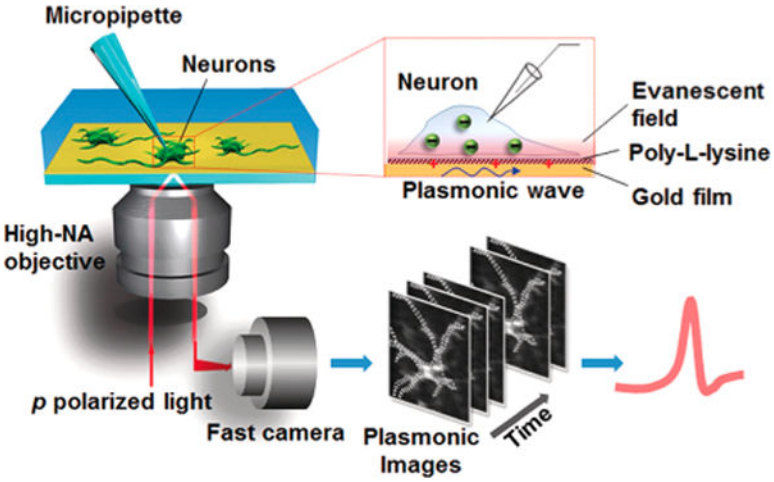

Figure 10.

Setup of plasmonic imaging of action potential in neurons. A *p*-polarized light beam is directed onto a gold-coated glass coverslip through an oil immersion objective to excited plasmons on the gold surface, which is imaged optically with a fast camera. Neurons are cultured on the poly-L-lysine-coated gold surface, and a micropipette is patched on one neuron to trigger action potential that is recorded with both the patch clamp electronics and plasmonic imaging. When an action potential spike is triggered, ions move in and out of the neuron via the ion channels, creating a transient charge near the gold surface, which affects surface plasmons on the gold film, which is imaged optically with P-EIM. Reproduced from Plasmonic-Based Electrochemical Impedance Imaging of Electrical Activities in Single Cells, Liu, X. W.; Yang, Y.; Wang, W.; Wang, S.; Gao, M.; Wu, J.; Tao, N. *Angew. Chem. Int. Ed.*, Vol. *56*, Issue 30 (ref [222]). Copyright 2017 Wiley.